SECURITY CLASSIFICATION OF THIS PAGE

(2)

DOCUMENTATION PAGE

Form Approved OMB No. 0704-0188

AD-A200 074

	1b. RESTRICTIVE MARKINGS: None
2b. DECLASSIFICATION / DOWNGRADING SCHEDULE: N/A	3. DISTRIBUTION / AVAILABILITY OF REPORT: Unlimited
4. PERFORMING ORGANIZATION REPORT NUMBER(S)	5. MONITORING ORGANIZATION REPORT NUMBER(S): AFOSR-TR-88-1017
6a. NAME OF PERFORMING ORGANIZATION: University of So. California	6b. OFFICE SYMBOL (If applicable):
6c. ADDRESS (City, State, and ZIP Code): Department of Electrical Engineering, Los Angeles, CA 90089-0241	7a. NAME OF MONITORING ORGANIZATION: AFOSR
	7b. ADDRESS (City, State, and ZIP Code): AFOSR/NE, Bolling AFB Washington, DC 20332
8a. NAME OF FUNDING / SPONSORING ORGANIZATION: AFOSR	8b. OFFICE SYMBOL (If applicable): NE
	9. PROCUREMENT INSTRUMENT IDENTIFICATION NUMBER: AFOSR-87-0273
8c. ADDRESS (City, State, and ZIP Code): AFOSR/NE, Bolling AFB Washington, DC 20332	10. SOURCE OF FUNDING NUMBERS: AFOSR-87-0273

PROGRAM ELEMENT NO	PROJECT NO	TASK NO	WORK UNIT ACCESSION NO
61102F	2306	B1	

11. TITLE (Include Security Classification): Investigations of the Optical and Electronic Properties of Crystalline Organic Materials

12. PERSONAL AUTHOR(S): Stephen R. Forrest

13a. TYPE OF REPORT	13b. TIME COVERED	14. DATE OF REPORT (Year, Month, Day)	15. PAGE COUNT
Annual	FROM 6/1/87 TO 5/14/88	August 22, 1988	27

16. SUPPLEMENTARY NOTATION

17. COSATI CODES		
FIELD	GROUP	SUB-GROUP

18. SUBJECT TERMS (Continue on reverse if necessary and identify by block number): Heterojunction, Molecular Semiconductor, Organic Semiconductor,

19. ABSTRACT (Continue on reverse if necessary and identify by block number)

A theory regarding transport of charge across crystalline molecular organic semiconductor/inorganic semiconductor heterojunctions is developed. It is found that transport under reverse bias, and under low forward bias is determined by carrier diffusion through the organic layer, and by thermionic emission across the heterojunction energy band discontinuity. Using the results of this theory, the valence band discontinuity energy between 3,4,9,10 perylenetetracarboxylic dianhydride and p-Si is directly measured using energy barrier photoemission spectroscopy and the analysis of the temperature dependence of the current-voltage data for this materials system. Apparently, this represents the first measurement of the band offsets between a molecular semiconductor and an inorganic semiconductor, and indicates the existence of relatively trap free heterointerfaces with many potential optical and electrical device applications. Additionally, an organic MBE system is described.

20. DISTRIBUTION / AVAILABILITY OF ABSTRACT	21. ABSTRACT SECURITY CLASSIFICATION
☒ UNCLASSIFIED/UNLIMITED ☐ SAME AS RPT ☐ DTIC USERS	Unclassified
22a. NAME OF RESPONSIBLE INDIVIDUAL: Dr. Stephen R. Forrest	22b. TELEPHONE (Include Area Code): (213) 743-6531
	22c. OFFICE SYMBOL: NE

DD Form 1473, JUN 86 — Previous editions are obsolete — SECURITY CLASSIFICATION OF THIS PAGE

Investigations of the Optical and Electronic Properties of Crystalline Organic Materials

Annual Report

June, 1987 - June, 1988

Contract: AFOSR-87-0273

Stephen R. Forrest

Departments of Electrical Engineering/Electrophysics

and Materials Science

University of Southern California

Los Angeles, CA 90089-0241

Investigations of the Optical and Electronic Properties of Crystalline Organic Materials

Annual Report

June, 1987 - June, 1988

Contract: AFOSR-87-0273

Stephen R. Forrest

Departments of Electrical Engineering/Electrophysics and Materials Science

University of Southern California

Los Angeles, CA 90089-0241

ABSTRACT

A theory regarding transport of charge across crystalline molecular organic semiconductor/inorganic semiconductor heterojunctions is developed. It is found that transport under reverse bias, and under low forward bias is determined by carrier diffusion through the organic layer, and by thermionic emission across the heterojunction energy band discontinuity. Using the results of this theory, the valence band discontinuity energy between 3,4,9,10 perylenetetracarboxylic dianhydride and p-Si is directly measured using energy barrier photoemission spectroscopy and the analysis of the temperature dependence of the current-voltage data for this materials system. Apparently, this represents the first measurement of the band offsets between a molecular semiconductor and an inorganic semiconductor, and indicates the existence of relatively trap free heterointerfaces with many potential optical and electrical device applications. Additionally, an organic MBE system is described.

TABLE OF CONTENTS

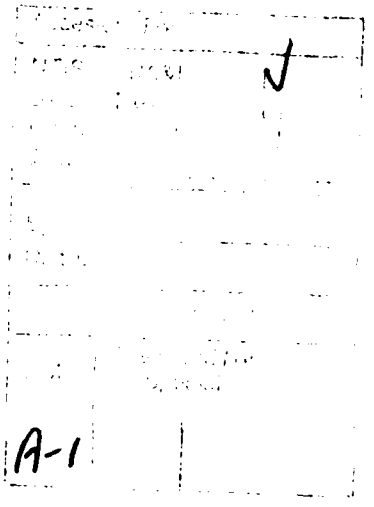

Summary of Technical Results

During the first year, two significant findings have been reported which indicate that organic-on-inorganic (OI) semiconductor heterojunctions are, in many ways, similar to fully organic heterojunctions. The first has been the theoretical understanding of transport across OI energy barriers. This analysis establishes diffusion to be the main mechanism for transport across the organic thin film. Applying this analysis to experimental data, it was then found that the diffusion velocity across several organic thin films is greater than 1000 cm/s. In related work, these results were further tested by measuring the optical response time of PTCDA (i.e. 3,4,9,10 perylenetetracarboxylic dianhydride)/p-Si avalanche photodiodes, and it was found that switching speeds as high as 1 GHz could be obtained.

Perhaps the most significant finding is that the first direct measurement of the valence band offset energy between such two dissimilar semiconductors (i.e. a crystalline molecular organic compound and a covalent semiconductor) was made using electron photoemission spectroscopy and analysis of thermionic emission across the heterojunction. These results point to a highly uniform, reproducible organic/inorganic heterojunction with few defect states. The significance of these results is that they give hope to the promise that the innumerable optical and electronic properties available to the broad family of crystalline (non-polymeric) organic semiconductors can be usefully employed in photonic devices and other heterojunction devices, without worrying about the constraints of lattice-match placed on conventional, inorganic heterojunctions.

In other related progress, an organic molecular beam epitaxy system has been constructed. Once it is fully instrumented, this system is designed to fabricate and probe (in situ) such structures as fully organic multiple quantum wells, waveguides, and heterojunction devices. The system has three evaporation/sublimation sources, and is outfitted with a cryopump, ion pump and Ti sublimation pump. Fixturing yet to be installed includes an *in situ* electrical/optical probing station, substrate temperature control for achieving very uniform, flat films, and in situ heterojunction processing for making two-level structures.

OI Heterojunction Theory and Measurement

To fully understand the physics of OI heterojunctions, a complete theory describing charge transport across OI HJs was developed. This theory differs in several ways from previous, somewhat incomplete theories developed to understand OI HJs. In particular, for the first time, the OI contact was considered to be a semiconductor/semiconductor HJ rather than a Schottky-like barrier. This picture is justified given that the organic compounds used are crystalline molecular semiconductors with moderate (2 eV) band gap energies. On the other hand, the bandwidths of the organic materials are small compared with inorganic semiconductors, and hence the transport through these former materials is dominated by injected charge rather than from bulk charge.

Nevertheless, using the HJ picture, it was realized that under reverse bias as well as low forward bias, charge is transported across the thin film (where the voltages are very small -- roughly 1 - 10 meV) via diffusion. Once the charge reaches the OI HJ barrier, it is thermionically emitted over the barrier, and then is swept out in the large electric fields developed across the inorganic semiconductor. This latter process has been described in detail in previous work involving OI devices. The parameter which best describes this transport process within the organic film is the "mean carrier velocity", $\langle v_c \rangle$, which replaces the Richardson constant commonly used for Schottky barrier devices.

The model leads to the immediate understanding of data obtained from several different experiments over the period of the last year. In particular, results from photoemission, time response, admittance and the forward current-voltage-temperature (I-V-T) characterisitics of OI HJ

diodes all can be understood both quantitatively and qualitatively in terms of this theory. The model also predicts the position of the quasi-Fermi Levels at the OI HJ as a function of forward and reverse voltage such that the OI device is now of greater use in understanding surface states at the OI interface. Using the model, it was possible to accurately determine the band discontinuity energy of an OI HJ consisting of PTCDA and p-Si. Some of these various data will now be discussed, along with their implications on the physics of organic/inorganic HJs. A more detailed presentation of results is given in the papers attached as Appendices I and II.

1) **Photoemission:** In Fig. 1 is shown the photocurrent spectrum of a PTCDA/p-Si diode for below-Si-bandgap light of wavelength between 1.2 μm and 3.2 μm. The peak centered at 2.2 μm is associated with carriers photoexcited over the OI HJ valence band discontinuity. The long wavelength tail of the peak yields a discontinuity energy of 0.50 eV, whereas the short wavelength cut-off is a result of the limited bandwidth of the organic semiconductor. To our knowledge, these data represent the first direct measurement of the band offset energies at the HJ between two such dissimilar semiconductors.

2) **I-V-T data:** It can be shown that the saturation current density for an OI HJ is given by:

$$J_S = J_O \exp(-q\phi/kT)$$

where J_O is a constant, q is the electronic charge, k is Boltzmann's constant, T is the temperature, and ϕ is the band discontinuity diffusion potential. Analysis of the forward I-V characteristics versus temperture can therefore be used to obtain the diffusion potential. This was done (Fig. 2), and from these data a band discontinuity energy for PTCDA/p-Si HJ's of 0.48 eV was determined. This independent measurement of the discontinuity energy is

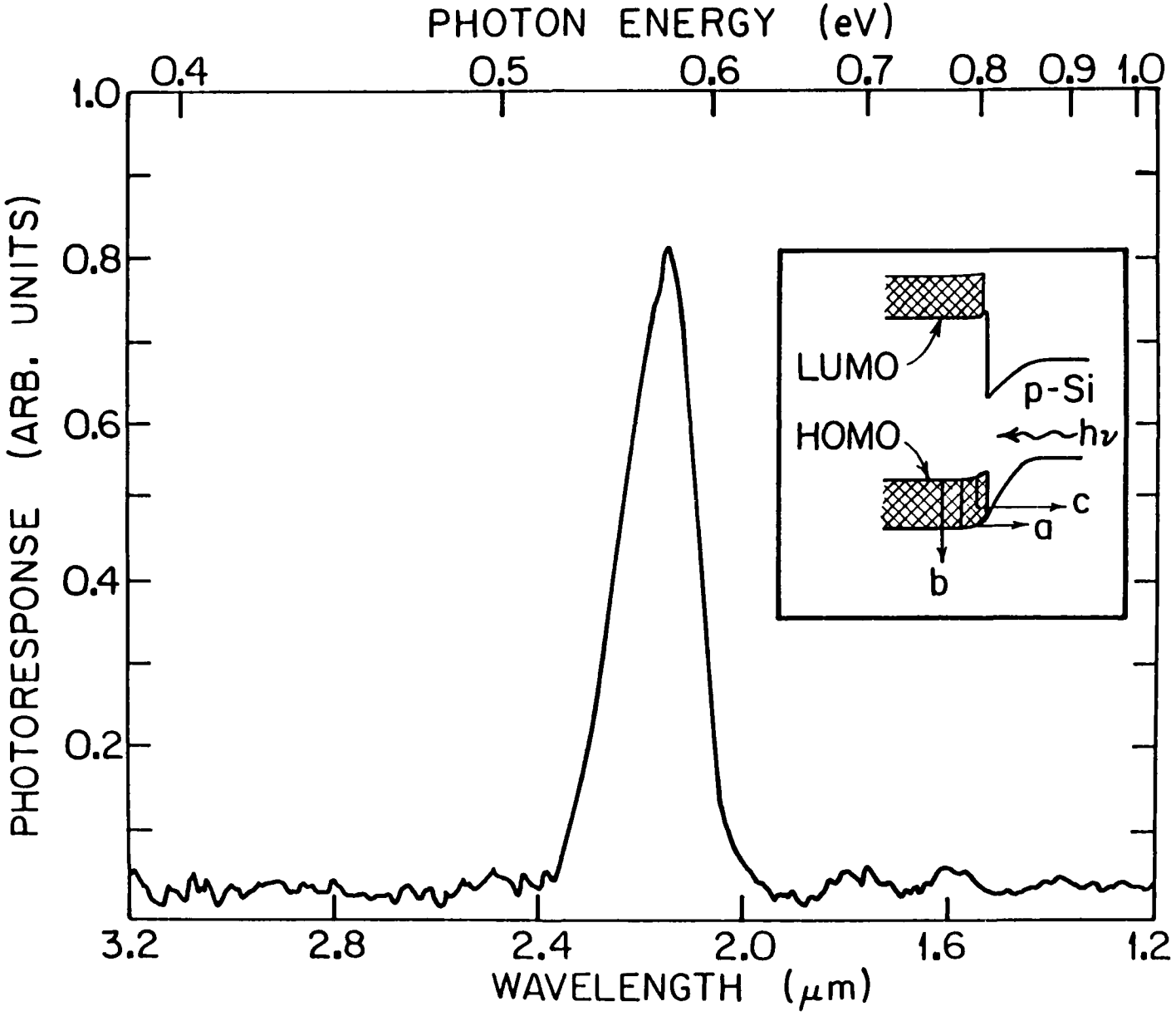
PHOTON ENERGY (eV)
0.4
0.5
0.6
0.7
0.8
0.9
1.0
PHOTORESPONSE (ARB. UNITS)
1.0
0.8
0.6
0.4
0.2
LUMO
p-Si
HOMO
hν
c
a
b
3.2
2.8
2.4
2.0
1.6
1.2
WAVELENGTH (μm)

Figure 1

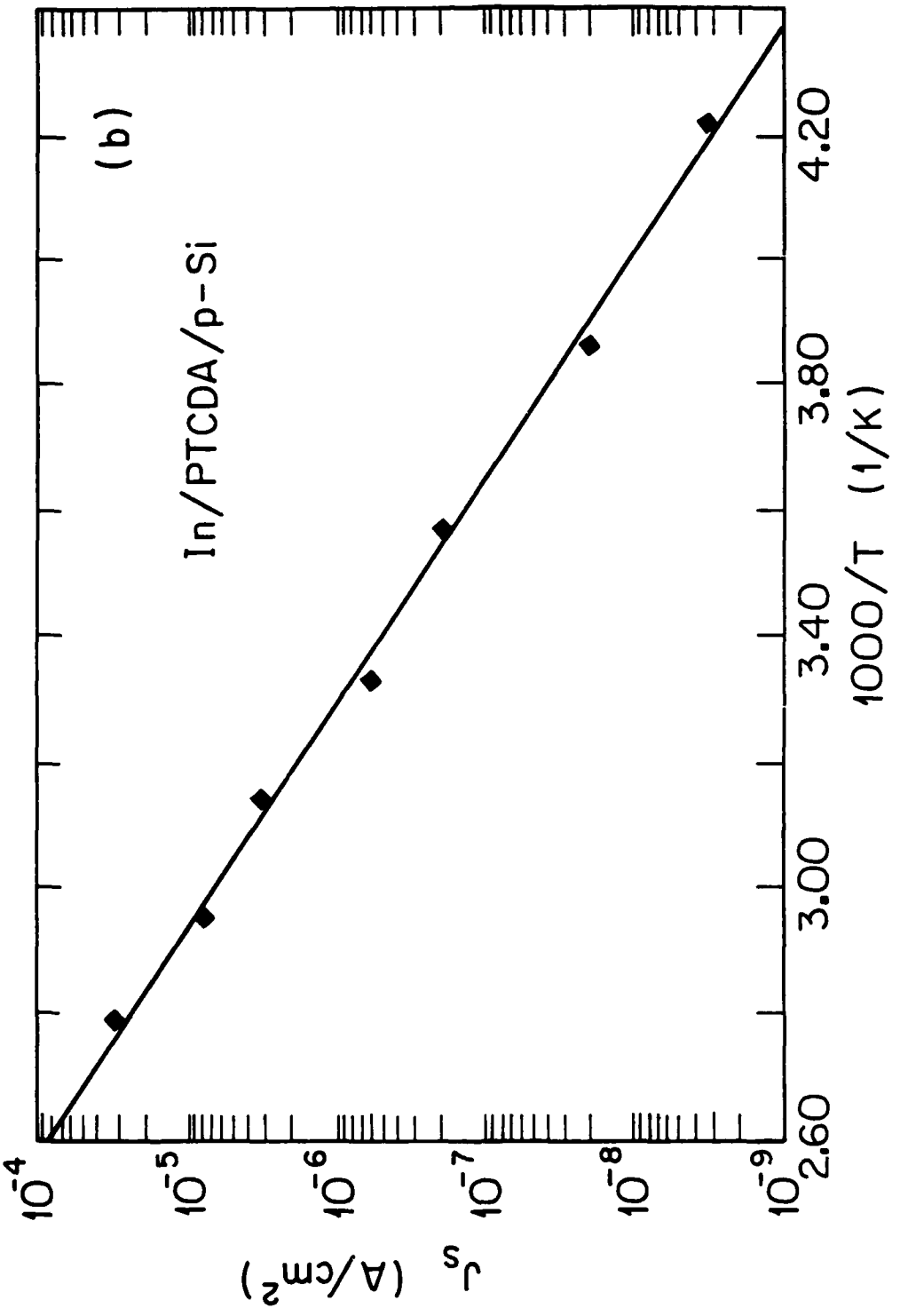
(b)
In/PTCDA/p-Si
J_s (A/cm^2)
10^{-4}
10^{-5}
10^{-6}
10^{-7}
10^{-8}
10^{-9}
2.60
3.00
3.40
3.80
4.20
1000/T (1/K)

Figure 2

consistent with photoemission data discussed above. Also, from the values obtained for J_0, it was also possible to obtain a value for the mean carrier diffusion velocity of > 500 cm/s, which is surprisingly high for organic semiconductors.

3) Semiconductor surface state analysis: Using the "correct" values for the band offsets along with calculations regarding the Fermi energy position at the HJ, it was possible to reanalyze earlier results regarding the position of surface defects incurred at OI HJ's. In earlier work, it was found that a high density of defects exist at the Si surface when Cu phthalocyanine (CuPc) is deposited onto that surface. It was theorized that the surface defects were a result of Cu being removed from the the CuPc and bonding to the Si. Due to the lack of an accurate measurement of the HJ band discontinuity energy, the deep level was presumed to exist at 0.5 eV above the Si valence band maximum (Fig. 3). Using the measured values for the barrier energy, this deep level was shifted to 0.7 eV -- a value consistent with Cu acceptors measured by other workers for bulk Si material.

4) Detector response time: In related work, an ITO/PTCDA/semiconductor (both Si and GaAs) photodetector was fabricated, and the speed of response of the diode to fast optical pulses whose wavelength was such that the light was absorbed in the inorganic substrate was measured. Using this device, it was found that a diode with a 2000Å thick organic film had a speed of response of 5 ns. This suggests a carrier diffusion velocity in the thin film of 3000 cm/s which is consistent with our HJ measurements. Furthermore, if a film of only 50Å is used, these detectors should have switching times as short as 100 ps, suggesting that they will find applications in many photonic system applications, as well as

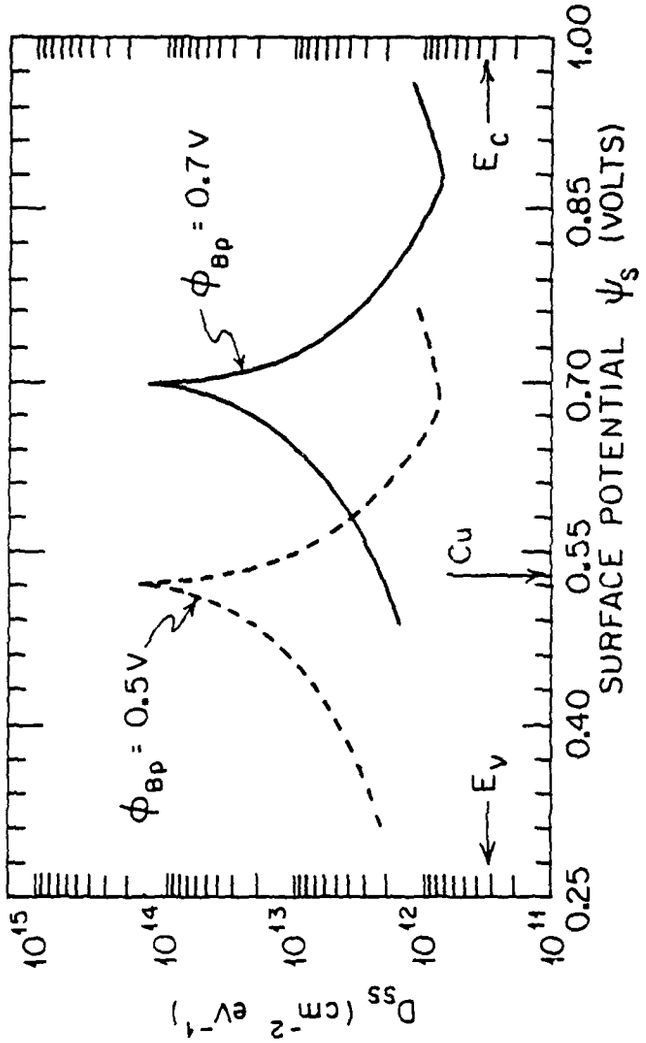
D_{ss} (cm^{-2} eV^{-1})
10^{15}
10^{14}
10^{13}
10^{12}
10^{11}
0.25
0.40
0.55
0.70
0.85
1.00
SURFACE POTENTIAL ψ_s (VOLTS)
ϕ_{Bp} = 0.5V
ϕ_{Bp} = 0.7V
E_c
E_v
Cu

Figure 3

for the analysis and detection of fast transient phenomena in inorganic substrate material.

Organic MBE

Highly uniform, smooth films with good interfaces are needed to study the nature of the OI HJ, as well as to understand transport across fully organic HJ's. In past work, standard diffusion pumped or ion pumped vacuum systems were relied upon for the fabrication of OI and fully organic HJ's. To enhance the ability to fabricate exotic structures, and to achieve highly uniform structures, this year an organic "molecular beam epitaxial" deposition system was fabricated. This apparatus is pumped by a combination of a cryopump, ion pump and Ti sublimation pump to achieve high vacuum. Three evaporation (sublimation) sources are provided for fabricating multi-layered structures. Furthermore, capability for depositing on hot or cold substrates (77 K to 600 K) is presently being installed. Most importantly, *in situ* processing of two level diode structures, as well as *in situ* optical and electrical probing of the devices without breaking vacuum will allow for the study of the OI and organic HJ's without worrying about the effects of uncontrolled atmospheric environments on device behavior. It is expected that this system will prove to be useful in the investigation and development of organic thin film semiconductors in the coming years.

Publications

Publications under AFOSR Sponsorship:

1. "Organic-on-Inorganic Semiconductor Heterojunctions: Energy-band Discontinuities, quasi-Fermi Levels, and Carrier Velocities", S. R. Forrest and F. F. So, J. Appl. Phys., 64, 399 (1988).

2. "Measurement of the Valence-band Discontinuities for Molecular Organic Semiconductor/Inorganic Semiconductor Heterojunctions", F. F. So and S. R. Forrest, Appl. Phys. Lett., 52, 1341 (1988).

3. "Investigation of Organic Heterojunctions", W. Y. Young and S. R. Forrest, manuscript in preparation for J. Appl. Phys.

Also, an invited paper on organic/inorganic semiconductor devices has been solicited by IEEE Circuits and Devices Magazine, which will be completed by the end of the summer.

Related publications:

1) "Growth and Characteristics of Organic-on-Inorganic Heterostructures", F. F. So and S. R. Forrest, SPIE Symposium on Advances in Semiconductors and Superconductors, Newport Beach, CA (1988). Talk and paper.

2) "A Fast Organic-on-Inorganic Semiconductor Photodetector", F. F. So and S. R. Forrest, Int. and Guided Wave Optics Tech. Dig., Santa Fe, NM (1988).

Personnel

P. I.: S. R. Forrest

Departments of Electrical Engineering and Materials Science

University of Southern California

Graduate Student: Franky F. So (3rd year).

Interaction with DoD Personnel

Numerous interactions between the group at USC and Air Force personnel regarding this research were pursued during the past year. In particular, the group at Hanscom AFB (A. Yang and J. Lorenzo) has had an ongoing interest in the OI HJ as a means of wafer analysis, as well as for its potential for active photonic device applications. Recently, two members of the Hanscom group (K. Vaccaro and A. Davis) visited the USC laboratory to learn more about the methods used in OI device fabrication and analysis such that these proceedures can be implemented at Hanscom. It is anticipated that the P.I. will be visiting Hanscom in the Fall, 1988 to further the progress of this "technology transfer". In addition, critical software has been provided to that laboratory to expedite analysis proceedures.

APPENDIX I

Measurement of the valence-band discontinuities for molecular organic semiconductor/inorganic semiconductor heterojunctions

F. F. So and S. R. Forrest

Departments of Electrical Engineering/Electrophysics and Materials Science & Engineering, University of Southern California, Los Angeles, California 90089-0241

(Received 30 December 1987; accepted for publication 15 February 1988)

Using the temperature dependence of the forward-biased current-voltage characteristics as well as internal photoemission, we directly measure the barrier potential and valence-band discontinuity energy (ΔE_v) of isotype heterojunctions formed between thin films of the crystalline organic semiconductor: 3,4,9,10-perylenetetracarboxylic dianhydride (PTCDA) and *p*-Si. We find $\Delta E_v = (0.50 \pm 0.02)$ eV. This, to our knowledge, is the first report of a measurement of a band discontinuity energy between a crystalline organic semiconductor and an inorganic semiconductor. These results are consistent with predictions of a current model involving diffusion and drift in the organic-on-inorganic (OI) semiconductor device. This model is employed to calculate ΔE_v using previously obtained barrier energies for several different PTCDA/inorganic semiconductor devices. In all cases, values of the barrier diffusion potential and ΔE_v are considerably smaller than apparent barrier energies obtained previously using pure thermionic emission theory to explain transport of charge over the OI barrier.

During the last several years, considerable interest has been focused worldwide on the study of semiconductor heterojunctions. The source of this interest lies in the ability of heterojunctions to control optical fields and charge transport in numerous devices such as semiconductor lasers and photodetectors used in optoelectronic applications. Furthermore, the ability to grow epitaxial materials with atomic scale precision has led to the realization of multiple quantum well structures which exhibit a wealth of exciting new physical phenomena, some of which are already finding novel device applications.

In addition to the more traditional heterojunctions being investigated, there have been a few reports of an entirely new class of heterojunctions[1-3] which are also finding interesting new applications,[4,5] and are leading to a greater understanding of semiconductors in general. These heterojunctions consist of organic (either crystalline molecular or disordered polymeric) semiconductors in contact with inorganic semiconductors. In this work, we present for the first time, measurement of the valence-band discontinuity energy between crystalline organic semiconductors and both elemental and compound inorganic semiconductor substrates. This differs from past work[1] in that the previous quantity measured was the "apparent barrier height," i.e., the heterojunction barrier energy inferred from the room-temperature, forward-biased current-voltage (I-V) characteristics using thermionic emission theory. While the apparent barrier height can be used to give a very accurate phenomenological model of transport across organic-on-inorganic semiconductor heterojunction (or OI-HJ) barriers, it is not successful in providing an accurate value for the energy-band discontinuities. Knowledge of these latter quantities, however, is central to our understanding of the physics underlying the formation of the OI-HJ barrier.

In the inset of Fig. 1 is shown a schematic cross section of an archetypal OI-HJ rectifier. The OI-HJ's consist of a thin (1000–2000 Å) layer of the purified crystalline organic dye: 3,4,9,10-perylenetetracarboxylic dianhydride (PTCDA) vacuum deposited onto inorganic semiconductor substrates using techniques described elsewhere.[4] The conductivity type of PTCDA is lightly *p* type. The inorganic semiconductor is Si, which is the material used in most of the studies to be discussed. The OI-HJ device is completed by making ohmic In contact to the substrate surface as well as to the organic thin film.

It has been shown[6] that the current density (J) is related to the voltage drop across the inorganic semiconductor (V_D) via

$$J = J_0 \exp(-q\phi_{B_p}/kT)[\exp(-qV_D/kT) - 1]$$
$$= J_s[\exp(-qV_D/kT) - 1]. \quad (1)$$

Here, k is Boltzman's constant, T is the temperature, q is the electronic charge, J_s is the saturation current, and ϕ_{B_p} is the OI-HJ barrier potential which may be voltage dependent. Also, we assume that the substrate is *p* type, in which case $V_D > 0$ for reverse bias. The value taken for J_0 strongly de-

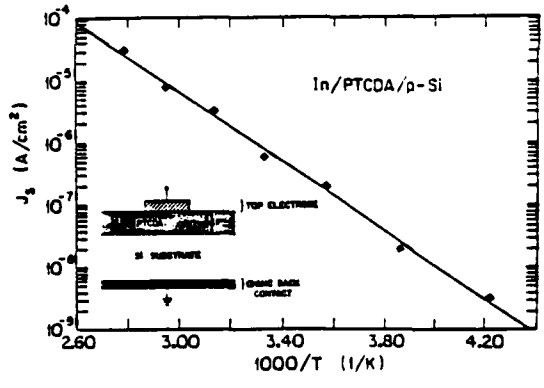

FIG. 1. Saturation current density (J_s) vs inverse temperature for an In/PTCDA/*p*-Si heterojunction. The solid line is a linear least squares fit to the data points. Inset: Schematic cross-sectional view of an organic/inorganic semiconductor heterojunction device.

 0003-6951/88/161341-03$01.00

pends on the mechanisms governing transport across the OI-HJ barrier. For example, it has often been assumed[1,2] that transport across the OI-HJ barrier is similar to that in a Schottky barrier diode and hence $J_0 = J_{SB} = A^* T^2$, where A^* is the Richardson constant. While this assumption is true for large forward bias, where a high density of charge is injected from the ohmic contacts into the organic thin film, it is not true under low forward or reverse voltage. In this bias regime, the very small hole concentration ($\sim 5\times 10^{14}$ cm^{-3}) in the organic thin film, coupled with its limited total density of states, suggests that diffusion and drift within the thin film will modify the value of J_0 from J_{SB}. Indeed, it can be shown[7] that for an OI-HJ diode

$$J_0 \cong J_{OI} = qN_v\langle v_c\rangle, \tag{2}$$

where N_v is the effective density of states at the inorganic semiconductor valence-band edge and $\langle v_c\rangle$ is the mean hole velocity in the organic thin film. Depending on the bias regime, $\langle v_c\rangle$ is determined either by hole drift (at moderate to high forward bias) or diffusion (at low forward or reverse bias). This latter case is typical for the conditions explored in this experiment. Assuming $\langle v_c\rangle$ is limited by diffusion, then $\langle v_c\rangle = (D_p/\tau_p)^{1/2} = (\mu_p kT/q\tau_p)^{1/2}$, where D_p is the diffusion constant, $\mu_p = 1$ cm^2/V s is the hole mobility of PTCDA,[5] and $\tau_p < 100$ ns is the hole lifetime obtained from current transient measurements.[3] For these conditions, $\langle v_c\rangle > 500$ cm/s, which is consistent with time-resolved measurements of the response of OI-HJ diodes to fast optical pulses.[9]

Note that typically $J_{SB} = 10^7$ A/cm^2. On the other hand, using $N_v = 2\times 10^{19}$ cm^{-3}, we obtain $J_{OI} \cong 2000$ A/cm^2, leading to $J_{OI}/J_{SB} = 2\times 10^{-4}$. In using the forward I-V characteristics to determine the apparent barrier height ϕ_{Bp}, one often measures the saturation current at $V_D = 0$ and equates that value to the prefactor to the term in square brackets in Eq. (1). Then, assuming a value (and hence a model) for J_0, one can extract the apparent barrier height. However, from the above discussion there would appear to be a large uncertainty in the value to use for J_0 in which case the actual barrier height cannot be determined with any reasonable accuracy. Indeed, without a direct measurement of the barrier height, one is also not capable of determining the valence-band discontinuity energy (ΔE_v). Thus, in our measurements we directly determine the barrier energy. Using this actual value for ϕ_{Bp}, J_0 is calculated giving a basis from which the appropriate model can be developed.

From Eq. (1) it is apparent that a measurement of the saturation current density (J_s) as a function of temperature can directly yield its activation energy ϕ_{Bp}.

Thus, a plot of $\log(J_s)$ as a function of $1/T$ is shown in Fig. 1. The device used had a contact area of 2.5×10^{-4} cm^2, and consisted of 2000 Å of PTCDA deposited on a 0.5 Ω cm (100) p-Si substrate.[9] A linear least squares fit to the data, as indicated by the straight line, gives $\phi_{Bp} = 0.56 \pm 0.02$ V and $J_0 = 1700$ A/cm^2. Note that both these values are considerably different from those obtained using thermionic emission theory,[1,6] where it was found that $\phi_{Bp} = 0.75$ V and $J_{SB} = 10^7$ A/cm^2. However, as indicated above, $J_0 \cong J_{OI} \cong 2000$ A/cm^2, in agreement with the model based on diffusion in the organic thin film.

The valence-band discontinuity energy for this isotype (p-P) heterojunction, ΔE_v, can be obtained from the actual (not apparent) value of ϕ_{Bp} using[10]

$$\Delta E_v = q\phi_{Bp} + \Delta_s - \Delta_o, \tag{3}$$

where Δ_s and Δ_o are the differences between the equilibrium Fermi energies and the valence-band maxima in the inorganic and organic semiconductor bulks, respectively. Using a hole concentration of $p_s = 5\times 10^{15}$ cm^{-3} and[8] $p_0 = 5\times 10^{14}$ cm^{-3} (where the subscripts "s" and "o" have the same meanings as used previously), with the effective hole mass (m^*) in the organic taken to be equal to the free-electron mass,[11] we obtain $\Delta E_v = (0.48 \pm 0.02)$ eV for PTCDA/p-Si heterojunctions. Note that PTCDA has a band-gap energy[4] of 2.2 eV, suggesting that $\Delta E_c = \Delta E_g - \Delta E_v \cong 0.6$ eV, where ΔE_g is the difference in band gaps between PTCDA and Si.

Although this analysis suggests that the actual barrier potential ϕ_{Bp} differs significantly from previously reported "apparent" values, the barrier height obtained from such transport measurements can lead to error in the presence of a high density of defect states at the heterojunction. While evidence from capacitance-voltage measurements[3,4] indicates a relatively low interface defect density for PTCDA/Si OI-HJ's, it is nevertheless worthwhile to utilize a more direct measurement of ΔE_v via internal photoemission.[11] In this experiment, a PTCDA/p-Si diode similar to that used in Fig. 1 was illuminated via the Si substrate using a 1-kHz chopped light source. In this manner, all light of energy ($h\nu$) greater than the Si band edge at 1.1 eV was eliminated from the OI-HJ region. To further attenuate the short wavelength radiation, a second Si wafer was interposed between the light source and the OI diode. The short-circuit photocurrent was then measured as a function of photon energy, resulting in the peak shown in Fig. 2(a) at $h\nu = 0.57$ eV.

The peak height was found to be insensitive to changes in both temperature and chopping frequency. In addition, to test whether the peak was due to excitation of traps in the bulk PTCDA, an In/PTCDA/indium tin oxide (ITO) photoconductor was fabricated. We found that no photoresponse was observed between $\lambda = 1$ and 3 μm for this device. Based on these observations, we can rule out the possibility that the peak is due to traps in the bulk semiconductors or at the OI-HJ interface.

We interpret this peak as follows. At $h\nu < 0.57$ eV, holes in the p-type organic thin film are excited above the OI-HJ, and are subsequently emitted over the barrier and collected in the external circuit [processes "a" and "c" in the inset of Fig. 2(a)]. Since this is the process of internal photoemission, the photocurrent at $h\nu < 0.57$ eV is expected to follow[12] $I_{PH} \propto (h\nu - \Delta E_v)^2$. Hence, Fig. 2(b) is a plot of $I_{PH}^{1/2}$ vs $h\nu$ for data taken on the long-wavelength side of the emission peak. A linear least squares fit to these data gives $\Delta E_v = (0.50 \pm 0.01)$ eV—a value in excellent agreement with that obtained using the foward-biased I-V characteristics in Fig. 1. Note, however, at $h\nu > 0.57$ eV, the data strongly deviate from that predicted for simple photoemission. At these

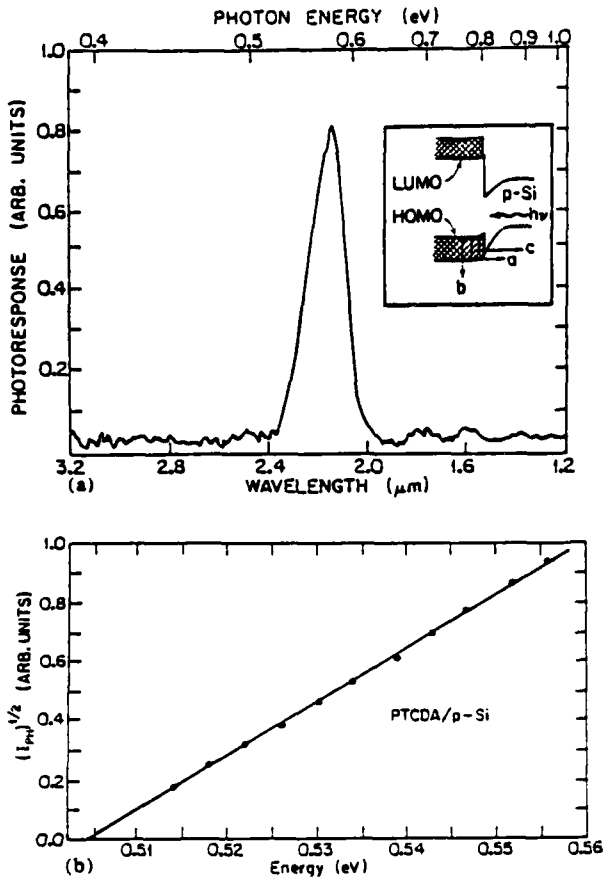

FIG. 2. (a) Photocurrent spectrum for an In/PTCDA/p-Si heterojunction illuminated via the p-Si substrate. The film thickness is 1000 Å. Inset: Band diagram of a PTCDA/p-Si heterojunction showing allowed ("a" and "c") and forbidden ("b") photoemission transitions resulting in the spectrum shown. (b) Square root of the photocurrent vs photon energy for the data on the long-wavelength side of the peak shown in (a). The solid line is a linear least squares fit to the data points.

high energies, I_{PH} drops with increasing $h\nu$. This effect can also be understood in terms of the band diagram in the inset of Fig. 2(a). Molecular semiconductors are characterized by narrow bandwidths,[13] as indicated by the cross-hatched region in the figure. For PTCDA, the total bandwidth bounded by the highest occupied molecular orbital (or HOMO) and lowest unoccupied MO (or LUMO) is only[4] 0.9 eV. Thus, transitions "b" beyond the bandwidth of the organic are forbidden, and hence a drop is expected in I_{PH} for this high-energy light.

Both of the experiments described above give support to a value of $\Delta E_v = (0.50 \pm 0.02)$ eV for PTCDA/p-Si heterojunctions, and for $J_0 = J_{OI}$ given by Eq. (2). With this confidence in determining J_0, we can calculate ΔE_v using Eqs. (1)–(3) for several PTCDA-based OI-HJ's where different inorganic substrates have been employed. Hence, in Table I, ΔE_v is listed for heterojunctions containing PTCDA along with Ge, GaAs, and GaSb using the apparent barrier height data of Ref. 1. In all cases, these values of ΔE_v are significantly smaller than their previously reported apparent values of ϕ_{Bp}.

TABLE I. Valence-band discontinuities for p-P PTCDA/inorganic semiconductor heterojunctions.

Inorganic substrate	J_{OI}/J_{SB}[a]	$q\phi_{Bp}$ (eV) TE[b]	Diffusion[c]	ΔE_v[d] (eV)
Si	1.4×10^{-4}	0.75 ± 0.02	0.56 ± 0.02	0.50 ± 0.02
Ge	6.6×10^{-3}	0.55 ± 0.03	0.30 ± 0.03	0.25 ± 0.04
GaAs	1.4×10^{-4}	0.75	0.52	0.43 ± 0.05
GaSb	1.2×10^{-4}	0.60	0.37	0.29 ± 0.04

[a]Assumes $\langle v_e \rangle = 500$ cm/s and $T = 300$ K.
[b]Values obtained for the apparent barrier height using thermionic emission (TE) theory from Ref. 1.
[c]Obtained using Eqs. (1) and (2) in text.
[d]Doping of Si and GaSb: 5×10^{15} cm^{-3}, Ge: 5×10^{14} cm^{-3}, and GaAs: 2×10^{16} cm^{-3}.

In conclusion, we have measured the barrier potential ϕ_{Bp}, and the valence-band discontinuity energy ΔE_v, for PTCDA/p-Si heterojunctions. These data are consistent with predictions of a model of hole transport in the devices which includes the effects of diffusion and drift in the OI diode. To our knowledge, this is the first report of the measurement of a band discontinuity energy for molecular organic/inorganic semiconductor heterojunctions, and the results further our understanding of these interesting structures.

The authors thank the Joint Services Electronics Program, the Air Force Office of Scientific Research, and Rome Air Development Center for support of this work.

[1]P. H. Schmidt, S. R. Forrest, and M. L. Kaplan, J. Electrochem. Soc. 133, 769 (1986).
[2]M. Ozaki, D. Peebles, B. R. Weinberger, A. J. Heeger, and A. G. MacDiarmid, J. Appl. Phys. 51, 4252 (1980).
[3]F. F. So and S. R. Forrest, J. Appl. Phys. 63, 442 (1988).
[4]S. R. Forrest, M. L. Kaplan, and P. H. Schmidt, Ann. Rev. Mater. Sci. 17, 189 (1987).
[5]C-L. Cheng, S. R. Forrest, M. L. Kaplan, and P. H. Schmidt, Appl. Phys. Lett. 47, 1217 (1986).
[6]S. R. Forrest, M. L. Kaplan, and P. H. Schmidt, J. Appl. Phys. 56, 543 (1984).
[7]S. R. Forrest and F. F. So, J. Appl. Phys. 63, June (1988).
[8]S. R. Forrest, M. L. Kaplan, and P. H. Schmidt, J. Appl. Phys. 55, 1492 (1984).
[9]F. F. So, S. R. Forrest, H. J. Garvin, and D. L. Jackson, *Integrated and Guided Wave Optics Technical Digest, Santa Fe, 1988* (Optical Society of America, Washington, DC, 1988).
[10]A. G. Milnes and D. L. Feucht, *Heterojunction and Metal-Semiconductor Junctions* (Academic, New York, 1972).
[11]Although setting m^* equal to the free electron mass (m_0) is a rough approximation, we note that $\Delta_0 \sim \ln(m^*/m_0)$. Hence, small deviations of m^* from m_0 are not expected to lead to significant inaccuracies in ΔE_v obtained from Eq. (3).
[12]M. A. Haase, M. A. Emanuel, S. C. Smith, J. J. Coleman, and G. E. Stillman, Appl. Phys. Lett. 50, 404 (1987).
[13]M. Pope and C. E. Swenberg, *Electronic Processes in Organic Crystals* (Clarendon, Oxford, 1982).

APPENDIX II

Organic-on-inorganic semiconductor heterojunctions: Energy-band discontinuities, quasi-Fermi levels, and carrier velocities

S. R. Forrest and F. F. So
Departments of Electrical Engineering and Materials Science, University of Southern California, Los Angeles, California 90089-0241

(Received 18 January 1988; accepted for publication 22 February 1988)

Organic-on-inorganic semiconductor heterojunctions (OI-HJs) exhibit rectification whereby the current-voltage characteristics are limited by the properties of the inorganic semiconductor substrate and the magnitude of the energy barrier at the heterointerface. In this paper we calculate the potential distribution and the quasi-Fermi level energy (or imref) across the OI diode bulk. Both ohmic as well as space-charge-limited conduction regimes of the organic thin film are considered. Previous work considered the OI-HJ to be similar to a Schottky, metal-semiconductor contact. While this can give a good approximation to OI-HJ transport processes under some bias regimes, it results in a misleading picture of the position of the imrefs under reverse bias, as well as errors in measurements of the band discontinuity energy at the OI-HJ. Unlike Schottky contacts, the imref in the OI diode is flat throughout the substrate under both low forward *and* reverse biases. These results are used to calculate carrier velocities within the organic film. The hole velocity is in the range of 100–2000 cm/s under reverse bias and is as high as 10^5 cm/s under forward bias. Experimental measurements of the energy-band discontinuities are presented that are in agreement with the predictions of the current-voltage model.

I. INTRODUCTION

The study of semiconductor heterojunctions has been a topic of great interest due to their ubiquitous use in numerous optical and electronic devices.[1] Indeed, the advent of optoelectronic devices employing multiple quantum-well heterojunction structures has led to entirely new classes of physical phenomena. This has resulted in the development of devices which perform highly complex and novel functions impossible to achieve with homogeneous semiconductor materials. Central to our utilization of these semiconductor-semiconductor contacts is the ability to accurately measure the magnitude of the energy-band discontinuities at the heterointerface.

Recently, investigations of a new class of heterojunctions, i.e., organic-on-inorganic semiconductor heterojunctions (OI-HJ), have attracted some interest[2,3] due to both the unusual nature of these contacts as well as to the potential new devices to which these heterojunction contacts can be applied. In particular, crystalline molecular semiconductors exhibit rectification when vacuum deposited onto inorganic semiconductor substrates,[2] and hence both the forward and reverse current-voltage characteristics exhibit properties limited by the magnitude of the OI-HJ band discontinuity and the properties of the bulk inorganic semiconductor material. As with fully inorganic semiconductor heterojunctions, it is essential that the energy-band discontinuities at the heterointerface be accurately determined in order that the mechanisms of charge transport across the energy barriers be fully understood. In the case of molecular semiconductor/inorganic-semiconductor heterojunctions, this has been done by analysis of room-temperature current-voltage characteristics, whereby an "apparent" barrier energy is measured which is generally larger than half the band gap of the underlying inorganic substrate.

In addition to determining the barrier height, it is important to understand the nature of the charge transport across the OI-HJ barriers. To do this, two essential quantities must be studied; the position of the nonequilibrium, or quasi-Fermi levels, and the carrier velocities throughout the heterojunction region. These quantities are of particular interest since a technique has been proposed whereby the surfaces of inorganic semiconductors such as InP, GaAs, and Si, can be electrically studied for the existence of surface states via the analysis of the quasistatic admittance properties of organic-on-inorganic heterojunction structures. The so-called semiconducting organic-on-inorganic surface analysis spectroscopic (or SOISAS) technique[4] is based on the assumptions that:

(1) The majority-carrier quasi-Fermi level at the OI-HJ is flat for small forward and reverse voltages. Quantitatively, this criterion should be loosely adhered to at applied voltages $|V_a| < E_g/2q$, where E_g is the band-gap energy of the inorganic semiconductor substrate and q is the electronic charge.

(2) The magnitude of the OI-HJ energy barrier is known to reasonable accuracy.

This technique was first applied[5] to InP and $In_{0.53}Ga_{0.47}As$ to evaluate the effects that various surface treatments have on the density of surface states. More recently, it has also been applied to Si as a means of determining whether various crystalline organic materials, such as 3,4,9,10 perylenetetracarboxylic dianhydride (PTCDA) and copper phthalocyanine (CuPc) react strongly with semiconductor surfaces.[6]

It is the purpose of this paper to calculate the potential distribution across all regions of the OI-HJ (Sec. II). This treatment departs from previous work in that (i) both ohmic and space-charge-limited (SCL) current regimes are consid-

 0021-8979/88/130399-11$02.40

ered in the organic thin film, and (ii) the effects of diffusion and drift in the thin film and substrate are discussed. These results are then used to determine the OI-HJ valence-band discontinuity energy between PTCDA and various inorganic semiconductors which heretofore has not been possible using previously reported "apparent" barrier energies. Data from several experimental tests of this theory are presented. In Sec. III we calculate the carrier velocities across the OI-HJ barrier. This is useful in understanding both the temporal response of the HJ, as well as in determining the majority-carrier quasi-Fermi level across the diode bulk, as is done in Sec. IV. In Sec. V we present conclusions concerning the implications of these results.

II. OI-HJ POTENTIAL DISTRIBUTION AND THE ENERGY-BAND DISCONTINUITIES

An OI-HJ device consists of a polycrystalline organic thin film vacuum deposited onto the polished surface of an inorganic substrate.[7] Typically, the organic film is between 100 and 5000 Å thick and can be layered onto either p- or n-type substrates with similar results. Metallic ohmic contacts are then made to both the organic and inorganic materials to complete the two-terminal device. It is observed that a rectifying heterojunction barrier is formed between certain crystalline organic dianhydrides (such as lightly p-type PTCDA) and many inorganic semiconductors. These heterojunction energy barriers determine the current-voltage characteristics of the complete device structure.

In analyzing charge transport across the OI-HJ barrier, we assume that the current in OI diodes is limited at low current levels by thermionic emission (TE) over the OI heterojunction band discontinuity, and at low bias by a combination of ohmic and trap-free space-charge-limited transport through the organic layer.[7] A band diagram of an isotype OI-HJ diode (assuming a p-type substrate) with a valence-band discontinuity energy of ΔE_v is shown in Fig. 1.

The potential distribution and the electric field (E) within the organic film are determined as a function of position (x) using Gauss' law. Thus, assuming single carrier (hole) injection:

$$\frac{dE}{dx} = \frac{q[p(x) - p_0]}{\kappa_0}, \tag{1}$$

where κ_0 is the permittivity of the organic thin film, p_0 is the free-hole concentration, and $p(x)$ is the total hole concentration consisting of the sum of p_0 and holes injected (p_{inj}) from the contact at $x = 0$. Assuming a constant mobility (μ_p) at small E, the current density within the film is

$$J = qp(x)\mu_p E(x), \tag{2}$$

which, via charge conservation, is independent of position (assuming no charge trapping). These equations have the following solution[8] for the voltage dropped (V_0) across an organic film of thickness t:

$$(q^3 p_0^3 \mu_p^2 V_0)/(\kappa_0 J^2) = u_t^2 - u_t - \ln(1 - u_t), \tag{3}$$

where

$$J = q^2 p_0^2 \mu_p t / \{[-u_t - \ln(1 - u_t)]\kappa_0\} \tag{4}$$

and

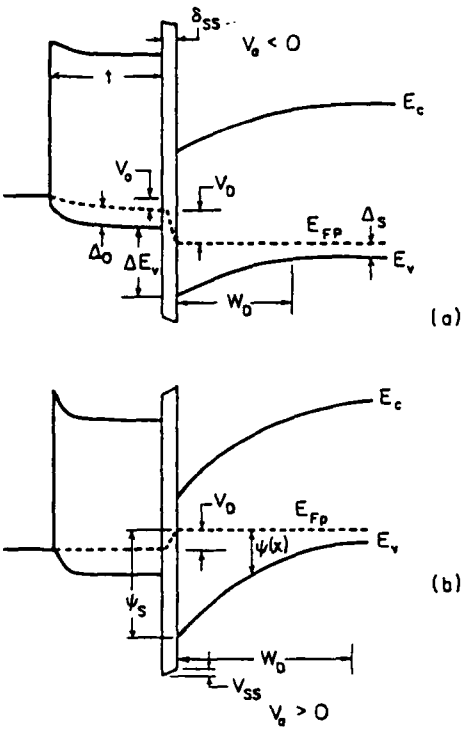

FIG. 1. Proposed energy-band diagram for an organic-on-inorganic semiconductor heterojunction device under (a) forward and (b) reverse bias.

$$u_t = p_0/p(t) \tag{5}$$

are related to the hole density at $x = t$. To solve Eqs. (3) and (4), we first choose a value of J from which the parameter, u_t, is determined via Eq. (4). This is substituted into Eq. (3), from which the voltage across the thin film, V_0, is calculated. The results of this calculation are shown in Fig. 2, where J is plotted as a function of V_0 for organic thin films with hole mobilities of $\mu_p = 0.01$ cm^2/V s and 0.1 cm^2/V s, a free-hole concentration of 5×10^{14} cm^{-3}, and a film thickness of 1000 Å. These values are typical of an OI diode using polycrystalline PTCDA as the organic layer.[7] In the figure, the ohmic transport regime at $V_0 < V_x \cong 0.02$ V (for $\mu_p = 0.01$ cm^2/V s) is distinguishable from the SCL regime at higher voltages. That is, at $V_0 < V_x$, $J \propto V_0$, whereas at $V_0 > V_x$, then $J \propto V_0^2$. This plot is in good agreement with observations of the J-V characteristics of metal/PTCDA/metal devices published earlier.[7] The important aspect of this plot is the low-current density ($J \lesssim 2$ mA/cm^2 for $\mu_p = 0.01$ cm^2/V s) at which ohmic gives way to SCL transport. Thus, at small forward voltages, and even at modest reverse biases for "leaky" OI diodes with small barrier diffusion potentials ϕ_{Bp}, the position of the hole quasi-Fermi level in the organic thin film is determined extrinsically by the amount of charge injected from the contacts (p_{inj}) rather than from the equilibrium concentration of carriers (p_0).

To calculate the potential distribution [$\psi(x)$] throughout the thin film, we replace V_0 by $\psi(x) < V_0 = \psi(t)$ in Eq. (3), and solve for $u(\ ) < u_t$. Then x is found using [cf. Eq. (4)]:

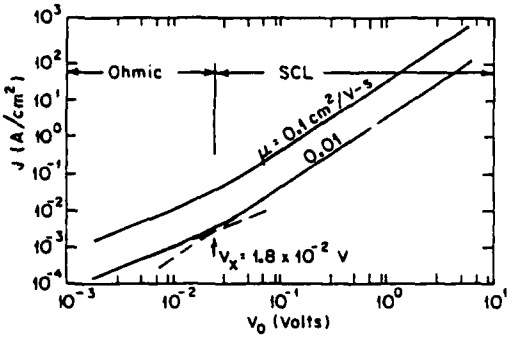

FIG. 2. Current (J) vs voltage (V_0) characteristics of a 1000-Å-thick organic film. The two curves correspond to films with mobilities of 0.1 and 0.01 cm^2/V s. Regions corresponding to ohmic and space-charge-limited (SCL) transport regimes are shown.

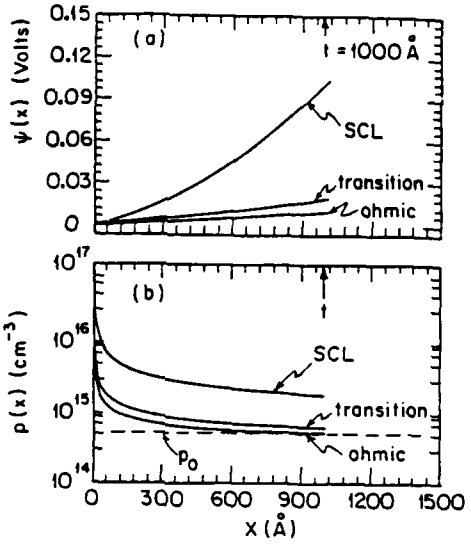

FIG. 3. (a) Potential distribution vs position within the organic thin film under three applied voltage regimes. The mobility of the 1000-Å-thick film is 0.01 cm^2/V s. (b) The free-hole distribution calculated for the film in 3(a). Here, p_0 corresponds to the equilibrium hole concentration.

$$q^2 p_0^2 \mu_p x/\kappa_0 J = -u(x) - \ln[1-u(x)]\,. \tag{6}$$

A plot of $\psi(x)$ is shown in Fig. 3(a) for the same film parameters as those used in Fig. 2, with $\mu_p = 0.01$ cm^2/V s. Note that $\psi(x)$ scales inversely with μ_p. Here, $\psi(x)$ is shown for three different voltages, V_0, corresponding to the ohmic, transition, and SCL regimes. In the transition regime, $V_0 \cong V_x$. As expected, in the ohmic regime the potential increases nearly linearly with distance from the metal contact at $x = 0$ to the OI heterointerface at $x = t$. However, even in the ohmic regime, there is some nonlinearity in $\psi(x)$ near $x = 0$ due to charge injection effects. In the SCL regime, the potential increase is nearly quadratic with distance, indicating a substantial amount of injected charge.

To determine the charge distribution as a function of x, the value of $u(x)$ for a given $\psi(x)$ and J is substituted into Eq. (5), which is then solved for $p(x)$. The results are shown in Fig. 3(b) for the same three regimes considered in Fig. 3(a). As expected, the charge piles up near the metallic cathode and decreases with distance toward the OI heterointerface where it reaches a minimum value of $p(t)$. In the ohmic regime, $p(t) \cong p_0$. For SCL transport, $p(t)$, which is the sum of the injected (p_{inj}) and background (p_0) carrier concentrations, can be considerably larger than p_0.

The current at the organic side of the heterojunction (at $x = t$) is given by

$$J(t) = J = q[p_s(V_D) - p_s(0)]\langle v_c\rangle\,, \tag{7}$$

where $p_s(V_D)$ is the hole density at the OI interface corresponding to the lowest point in the valence-band maximum at the inorganic-semiconductor surface (Fig. 1). Also, V_D is the voltage drop across the inorganic substrate. Equation (7) suggests that current injected from the substrate into the organic thin film is limited by the rate at which carriers are transported toward the contacts. This limit is determined by the mean carrier velocity, $\langle v_c\rangle$, within the organic film, and at low V_0 is approximately given by

$$\langle v_c\rangle = v_{c0} = V_0\mu_p/t\,. \tag{8}$$

Equation (8) is the drift velocity in the ohmic regime where diffusion is neglected (see below), and once again assumes μ_p is independent of E. At higher voltages it is more appropriate to use the full expression for the mean carrier velocity, viz:

$$\langle v_c\rangle = \frac{1}{t}\int_0^t v_c(x)dx = \frac{1}{t}\int_0^t \mu_p(x)E(x)dx\,. \tag{9}$$

We note that the above treatment considers only drift. However, diffusion becomes important at $V_0 \lesssim kT/q$. Since V_x is approximately equal to the thermal, or diffusion potential, this suggests that diffusion is important under some (low voltage) diode operating conditions. When diffusion of holes in the organic layer is significant, the drift velocity is replaced by

$$\langle v_c\rangle = (D_{p0}/\tau_{p0})^{1/2} = (\mu_p kT/q\tau_{p0})^{1/2}\,, \tag{10}$$

where D_{p0} and τ_{p0} are the diffusion constant and lifetime of holes within the organic thin film, respectively. It has recently been found[9] that $\tau_{p0} < 10^{-7}$ s in PTCDA, suggesting a minimum carrier velocity due to diffusion through the thin film of 500 cm/s for $\mu_p = 1$ cm^2/V s.

The current on the inorganic side of the heterojunction is given by

$$J = qD_{ps}\left(\frac{qpE}{kT} - \frac{dp}{dx}\right), \tag{11}$$

where D_{ps} is the diffusion constant for holes in the inorganic-semiconductor substrate and E is the electric field. This equation is solved using Eq. (7) along with:

$$p(x) = N_{vs}\exp[-q\psi(x)/kT]\,, \tag{12}$$

where $\psi(x)$ is the energy difference between the valence-band maximum and the substrate quasi-Fermi level (Fig. 1), and N_{vs} is the effective valence-band density of states for the inorganic material.

Using Eqs. (7), (11), and (12) gives

$$J = [qN_{us}\langle v_c\rangle/(1+\langle v_c\rangle/v_d)] \times \exp(-q\phi_{Bp}/kT)[\exp(-qV_D/kT)-1]. \quad (13)$$

Here, ϕ_{Bp} is the diffusion potential due to the OI-HJ barrier and v_d is the inorganic material diffusion velocity given by

$$v_d = D_{ps}\left[\int_t^{W_D+t}\exp\left(\frac{q[\phi_{Bp}-\psi(x)]}{kT}\right)dx\right]^{-1}, \quad (14)$$

where W_D is the depletion region width.

We now express the barrier diffusion potential, ϕ_{Bp} in terms of the valence-band discontinuity energy ΔE_v. For isotype heterojunctions[1]:

$$\Delta E_v = q\phi_{Bp} + \Delta_s - \Delta_0, \quad (15)$$

where Δ_s and Δ_0 are the energy differences between the equilibrium Fermi levels in the bulk of the semiconductor substrate and organic thin film, respectively. That is, for the inorganic material:

$$\Delta_s = -kT\ln(p_s/N_{us}), \quad (16)$$

where p_s is the equilibrium hole concentration. An expression similar to Eq. (16) is also used to determine Δ_0.

Equation (15) implies that, under certain conditions, ϕ_{Bp} is bias dependent. Since the equilibrium carrier concentration, p_0, in the organic layer is relatively small in many crystalline organic compounds, then under conditions of large injected currents where $p_{inj} \gg p_0$, the value of Δ_0 can change significantly from its equilibrium value. As ΔE_v is an intrinsic property of the HJ which is unaffected by the presence of injected charge, we therefore conclude that ϕ_{Bp} must also be bias dependent. This dependence is in addition to relatively small[10] image force lowering of ϕ_{Bp}. In effect, when $p_{inj} \gg p_0$, Δ_0 must decrease, thereby inducing a corresponding decrease in ϕ_{Bp}. This effect is very pronounced in OI diodes, whereas in Schottky devices it is negligible due to the large free-carrier concentration in the metal contact. Thus, Eq. (13) is similar to that which is obtained in the case of Schottky barriers,[11] with the exception that for OI devices ϕ_{Bp} can be voltage dependent under strong, forward biased current injection. Also, $\langle v_c\rangle$ is used in place of v_c, i.e., the "collection" velocity of the metal contact. Nevertheless, if ϕ_{Bp} is measured under low injection conditions, the valence-band discontinuity energy (or conduction-band discontinuity, ΔE_c, in the case of n-type substrates) can be inferred using p_0.

Equation (13) is also similar to the results obtained for thermionic emission over the OI barrier,[7] except that the exponential prefactor for TE limited currents used in previous work is simply A^*T^2, where A^* is the Richardson constant. If J_{SB} is the current due to thermionic emission over a Schottky-like OI barrier, and recognizing that in most cases $\langle v_c\rangle/v_d \ll 1$ (Sec. III), then

$$J/J_{SB} = \langle v_c\rangle(2\pi m^*/kT)^{1/2}, \quad (17)$$

where m^* is the effective mass of holes in the inorganic substrate. Taking $\langle v_c\rangle = 10^3$ cm/s (see Sec. III), $m^* = m_0$ (where m_0 is the electron rest mass), and $T = 300$ K, we obtain $J/J_{SB} \cong 3.7\times10^{-4}$. As the forward bias is increased, $\langle v_c\rangle$ is also increased [Eq. (9)]. In this case, J/J_{TE} approaches 1, implying that the conduction mechanism under strong forward injection approaches that of an ideal Schottky diode. Here, the organic material becomes degenerate due to the presence of a high density of injected charge, and hence its behavior approximates that of a metal contact. Indeed, the ratio J/J_{SB} is a qualitative measure of the validity of the use of the Schottky approximation in analyzing OI diode transport. Clearly, this approximation fails at low current injection, where $\langle v_c\rangle$ becomes small.

Using these current-voltage relationships, we can calculate the potential distribution across the entire OI diode, assuming that there is no significant charge trapping in the device volume. In this case, Eqs. (4) and (13) are equal. Furthermore, the applied voltage is given by[4]

$$V_a = V_D + V_{ss} + V_0 \cong nV_D + V_0, \quad (18)$$

where V_{ss} is the voltage drop across any interfacial (oxide or trap) layer existing between the organic and inorganic layers, respectively, and $n > 1$ is the n value in the exponential voltage dependence of the dark current under forward bias.

In Fig. 4 we plot the various forward biased component voltages as a function of V_a, assuming two values of OI barrier height. Other parameters used in this calculation are similar to those in Fig. 3. Also, we take $n = 1.5$, $T = 300$ K, $N_{us} = 2\times10^{19}$ cm^{-3} for p-Si, and $\langle v_c\rangle$ is given by the greater of Eq. (9) or (10), which is a function of the voltage drop across the organic thin film. As expected, at low forward bias the voltage is predominantly dropped across the inorganic substrate (i.e., $V_D > V_{ss}, V_0$). At higher voltages, SCL transport through the organic layer dominates, leading to a larger voltage drop across the organic thin film. The shift between ohmic and SCL transport in the film is evidenced by the change in slope in the curves at the value of V_a where all the voltage components are approximately equal. Below this transition point, we expect the J-V characteristic to depend exponentially on $V_a \cong V_D$ as indicated by Eq. (13). At higher voltages, $V_a \cong V_0$, and in this case $J \propto \sim V_a^2$, typical of SCL transport. Note that the transition from TE to SCL dominated currents occurs at lower values of V_a as the OI barrier height is decreased. This results since the current is higher at a given voltage as the barrier height is lowered [cf. Eq. (13)].

Under the reverse bias, V_0 and V_{ss} are considerably smaller than V_D due to the small leakage currents character-

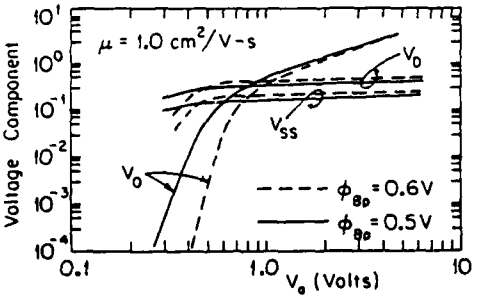

FIG. 4. Component voltages vs applied voltage for a forward biased OI-HJ diode, assuming two different barrier potentials of 0.6 and 0.5 V. Here, V_D, V_{ss}, and V_0 correspond to the voltage across the substrate depletion region, interfacial region, and thin film, respectively. A film thickness of 1000 Å is assumed.

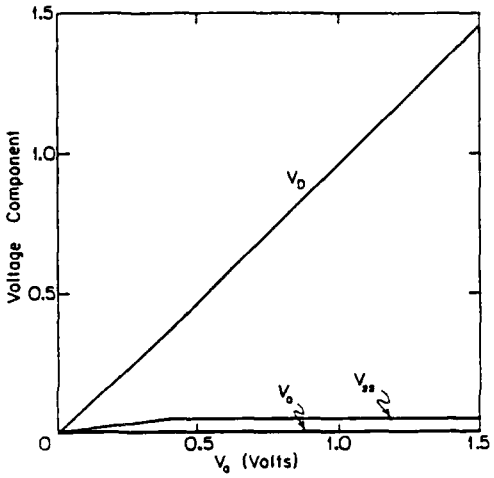

FIG. 5. Component voltages vs reverse applied voltage for the device in Fig. 4.

istic of OI-HJ structures. The division of voltages in reverse biased devices has been treated in detail elsewhere,[4] and hence is shown for only a single set of conditions in Fig. 5 for reference.

The validity of the assumptions leading to the expression for current density [Eq. (13)] needs to be tested. This is particularly important since the magnitude of J/J_{SB} in Eq. (17) is significantly less than one, such that large errors in determining the barrier energy from the forward current-voltage characteristics can be incurred. To distinguish between the diffusion and thermionic models, we note that the total saturation current density, J_s, is given by

$$J_s = J_0 \exp(-q\phi_{Bp}/kT), \tag{19}$$

where J_0 is equal to either the prefactor in Eq. (13), or in the case of pure thermionic emission, $J_0 = A^*T^2$. Thus, a plot of $\log(J_s)$ vs $1/T$ should be nearly exponential, with small deviations due to the weak temperature dependence of J_0. The slope of this plot gives the barrier energy and the intercept with the $\log(J_s)$ axis yields $\log(J_0)$.

In Fig. 6(a) is shown the temperature dependence of the forward biased J-V characteristics of an In/PTCDA/p-Si device (cf. Fig. 4, Ref. 12). From the intercept of these curves with the $V_a = 0 = V_D$ axis, we obtain the saturation current as a function of T, which is replotted in Fig. 6(b). The saturation current density is thermally activated, and a least-squares fit to the data—as indicated by the solid line—gives $\phi_{Bp} \approx 0.56 \pm 0.02$ V and $J_0 = 1700$ A/cm^2. This value for the barrier height is significantly smaller than the "apparent" values obtained using thermionic emission, where $\phi_{Bp} = 0.75$ V is typical for these diodes. Furthermore, $J_0 = A^*T^2 = 9\times10^6$ A/cm^2 for p-Si Schottky diodes, which is several orders of magnitude larger than the value of J_0 actually obtained. Returning to Eq. (13), we see that for $\langle v_c\rangle/v_d \ll 1$, then $J_0 = qN_{vs}\langle v_c\rangle$. Using $J_0 = 1700$ A/cm^2, and $N_{vs} = 2\times10^{19}$ cm^{-3} for p-Si, then $\langle v_c\rangle = 450$ cm/s. This is in satisfactory agreement with the lower limit value of 500 cm/s previously estimated using carrier lifetime data.

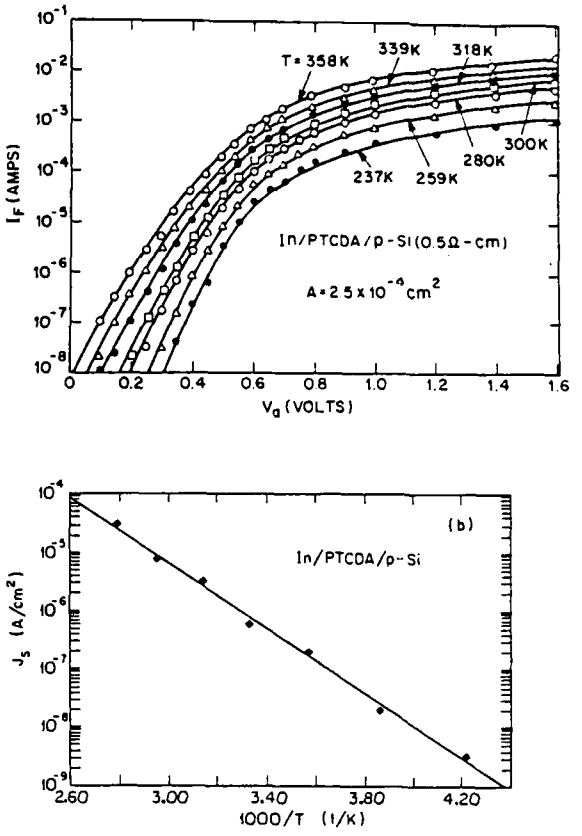

FIG. 6. (a) Forward current-voltage characteristics of an In/PTCDA/p-Si diode measured at several different temperatures (cf. Ref. 12). The PTCDA thickness is 2000 Å. (b) Saturation current density vs $1/T$ for the diode in (a). The solid line represents a best fit to the data, and gives a barrier diffusion potential of $\phi_{Bp} = 0.56$ V, and an intercept with the J_s axis of $J_0 = 1700$ A/cm^2.

This result is therefore in strong support of the model of current transport across the OI-HJ barrier limited by both diffusion and drift [Eq. (13)]. Using $\phi_{Bp} = 0.56 \pm 0.02$ V along with Eq. (15), a valence-band discontinuity energy for PTCDA/p-Si devices of $\Delta E_v = (0.48 \pm 0.02)$ eV is obtained. To our knowledge, this represents the first such measurement of an energy-band discontinuity in crystalline organic/inorganic semiconductor heterojunctions.

The values for ϕ_{Bp} obtained through the use of Eq. (13) are still subject to errors induced by approximations used in developing the transport model. In particular, although there is no direct evidence of a high density of surface charge,[6] one would expect that such interfacial defects could affect the measurement of ΔE_v using J-V analysis. Therefore, ΔE_v was also measured via internal photoemission.

In Schottky[13] or isotype heterojunction[1,14] barriers, free majority carriers can be photoexcited over the barrier by sub-band-gap energy photons. The photocurrent (I_{ph}) induced per photon absorbed is given by[15]

$$I_{ph} \propto (h\nu - \Delta E_v)^2, \tag{20}$$

where h is Planck's constant and ν is the frequency of the

incident light. To directly measure ΔE_v in OI-HJ devices, the photoemission current spectrum for a PTCDA/*p*-Si diode was investigated. For this experiment, the diode was fabricated in the same manner as that used in obtaining the data in Fig. 6. This diode was placed perpendicular to a chopped (1 kHz) monochromatic light source incident via the substrate such that light with $h\nu$ greater than the band gap of Si was filtered out before reaching the diode active area at the OI interface. To further suppress the signal due to the fundamental absorption in Si, a second Si wafer was placed between the light source and the OI diode. The band gap[7] of PTCDA is 2.2 eV, such that no direct absorption in the organic material is expected in this experiment.

The resultant photoresponse as a function of light energy and wavelength is shown in Fig. 7(a). In obtaining these data, the OI diode was operated at $V_a = 0$. A maximum response is clearly observed in the photoemission spectrum at 0.57 eV. No signal is observed between the energy of this peak and the band edge of Si. The peak height did not change with temperature (varied from 20 to 100 °C) or light chopping frequency (varied from 100 Hz to 2 kHz). Furthermore, the peak was unaffected by strong white light illumination (or bleaching) incident on the thin-film surface. Finally, an In/PTCDA/indium-tin-oxide device was also fabricated and illuminated in the same wavelength region as the In/PTCDA/*p*-Si sample. However, the former device had no photoresponse peak as that shown in Fig. 7(a), indicating that the peak is not due to a photoemission process in the PTCDA itself. These observations, coupled with the relatively high intensity of the signal, rule out the possibility that the peak is due to a high density of traps in the semiconductor bulks or at the OI-HJ interface.

We attribute this response to the photoemission of carriers from the highest occupied molecular orbital (or HOMO) in PTCDA to the valence-band maximum in *p*-Si over the interface barrier energy. However, note that the signal shown in Fig. 7(a) is considerably different than that predicted for photoemission, where we expect a monotonic increase in I_{ph} with energy. The dip in the OI-HJ photoemission data at high energy can be understood in terms of the band diagram in the inset of Fig. 7(a) where the widths of the organic energy bands are indicated by the crosshatched regions.[16] Unlike Schottky diodes or inorganic semiconductors, molecular semiconductors are characterized by relatively narrow bands, with a high density of states within those bands. Optical absorption experiments[7] have shown that the total HOMO plus LUMO (lowest unoccupied molecular orbital) bandwidth is 0.9 eV for PTCDA. If we now assume that the valence bandwidth is on the order of ΔE_v, then the peak absorption occurs at photon energies comparable to this barrier height [processes "*a*" and "*c*" in the inset of Fig. 7(a)]. However, as the photon energy increases the transitions are forbidden in the organic material as a result of the narrow bandwidth (process "*b*"), and hence a decrease in I_{ph} with increasing $h\nu$ is observed. Finally, for $h\nu < \Delta E_v$, the photon has insufficient energy for photoemission to occur.

From these arguments, the photocurrent on the long wavelength side of the peak should follow Eq. (20). Thus, in

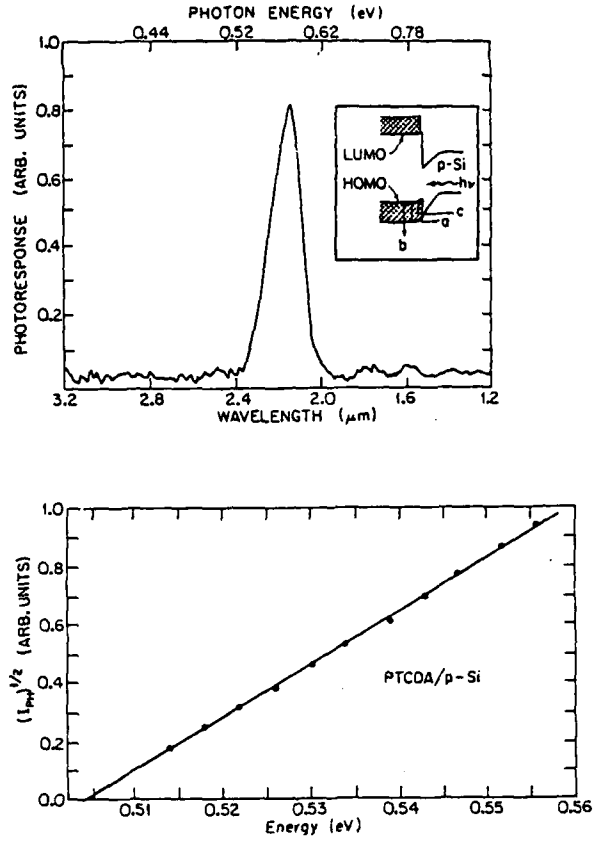

FIG. 7. (a) Photoemission spectrum of an In/PTCDA/*p*-Si heterojunction diode. Inset: Band diagram of the OI-HJ showing the allowed emission processes ("*a*" and "*c*") and the forbidden, high-energy process "*b*." The crosshatched regions refer to width of the organic bands. (b) The square root of the photocurrent on the long wavelength branch of the response peak in (a) plotted vs photon energy. The intercept of the straight line fit to the data with the $(I_{ph})^{1/2} = 0$ axis gives $\Delta E_v = (0.50 \pm 0.01)$ eV.

Fig. 7(b) we plot $(I_{ph})^{1/2}$ vs photon energy ($h\nu$), and find that the dependence is linear along nearly the entire long wavelength edge. The intercept of these data with the energy axis gives $\Delta E_v = (0.50 \pm 0.01)$ eV, a value consistent with that obtained from the *J-V* analysis.

Accurate determination of the barrier height as provided above has important implications as to the interpretation of the mechanisms affecting the formation of OI-HJ contact barriers. For example, as discussed in Sec. I, measurements of the density of interface states using the SOISAS technique are affected by the value of the OI-HJ barrier energy. In Fig. 8 is shown the density of states in equilibrium with a *p*-Si substrate (D_{ss}) as a function of energy in the Si band gap for a Cu-phthalocyanine/*p*-Si OI-HJ. The solid line corresponds to the data assuming an apparent barrier height of 0.70 V as determined from thermionic emission theory,[6] and the dashed line is this same data replotted assuming a barrier height of 0.50 V, which would be obtained from Eq. (13), assuming the hole velocity in Cu-phthalocyanine (CuPc) is approximately the same as that in PTCDA. This latter as-

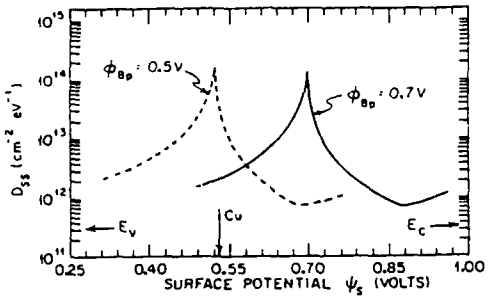

FIG. 8. Density of surface states (D_{ss}) vs potential at the Si surface for a CuPc/p-Si heterojunction. The solid line refers to data from Ref. 6 using a barrier height of 0.7 V. The dashed line is for this same data except that $\phi_{Bp} = 0.5$ V estimated using the OI-HJ current model. The arrow labeled "Cu" corresponds to the position of the Cu acceptor defect level in bulk Si. Also, E_c and E_v refer to the conduction and valence-band extrema in Si, respectively.

sumption is justified by the nearly equal hole mobilities of these two organic compounds. Thus, the position of the trap density curve is linearly related to the barrier energy.

We note that the large peak value for D_{ss} for CuPc/p-Si OI-HJs has been attributed[6] to reactions between these two materials at the heterointerface, resulting in free Cu at the Si surface. The corrected data appear to support this model, since the peak in D_{ss} nearly coincides with the Cu acceptor defect energy of 0.52 eV above the valence-band maximum in Si.[17] The position of this Cu defect is indicated by the vertical line in Fig. 8. Hence, knowledge of the actual, rather than the apparent values for ϕ_B is central to our understanding of the OI-HJ barrier.

For purposes of comparison, OI-HJ energy barrier heights measured assuming both thermionic emission and diffusion-limited transport models are given in Table I. These data are for PTCDA-based OI-HJ diodes only, and are taken from Ref. 2. Also included in the table are values of ΔE_v for selected OI-HJs as inferred from the diffusion model values of ϕ_{Bp} using Eq. (15).

III. CARRIER VELOCITIES

The carrier velocity $\langle v_c \rangle$ in the thin film is determined using Eqs. (9) and (10). The results for forward biased devices are given in Fig. 9. Here, the velocity is plotted for several values of thin-film hole mobility ranging from 0.01 to 1 cm^2/V s, and for two values of ϕ_{Bp} (cf. Fig. 2 for other parameters used). It is apparent that the carrier velocity strongly depends on voltage, V_D, with $\langle v_c \rangle$ increasing exponentially when $V_D > 0.3$ V. Velocities as high as 10^5 cm/s are expected for thin films with high mobilities, and for diodes with barrier heights of 0.50 V. The dependence of these curves on V_D is a result of the increase of $\langle v_c \rangle$ with voltage V_0, when $V_0 > kT/q$. At low voltage, the electric field in the thin film is small, such that diffusion dominates. In this case, $\langle v_c \rangle$ is given by Eq. (10), where $\tau_p = 1.0\,\mu$s was assumed in these calculations. As V_D increases beyond 0.3 V, the voltage drop across the thin organic film increases due to the transition into the SCL current regime. The velocity at a given voltage decreases as the barrier height increases due to the reduced forward current, hence resulting in a lower voltage drop across the thin film.

The above treatment assumes a constant hole mobility in the organic crystal, independent of the magnitude of the applied electric field. The relatively high mobility of holes arises from the large overlap of electronic wave functions in the s-p orbitals of adjacent molecules in a crystalline stack. At the highest electric fields, it is expected[18,19] that the mobility will decrease somewhat due to the increased generation of phonons. Such processes depend on temperature, crystallinity, and film purity, and need to be taken into consideration; especially under large forward bias.

Under reverse bias, the electric field in the thin film is small, such that the drift velocity is much smaller than the diffusion velocity [Eq. (10)] for all but the smallest values of ϕ_{Bp}. Hence, under reverse bias, $\langle v_c \rangle$ varies from 100 cm/s to approximately 2000 cm/s, depending on the mobility and lifetime of holes in the organic layer. For these conditions the film will respond to even low-frequency signals as if it were a leaky dielectric in a metal-insulator-semiconductor (MIS) capacitor. However, due to the high conductivity of the thin film compared with that of glassy insulators such as SiO_2, it is not possible to strongly invert the surface of the OI diode. As greater reverse voltages are applied such that the Fermi level at the OI interface is brought to well above the center of the inorganic semiconductor band gap, the minority carriers (electrons) arriving from the semiconductor bulk are either

TABLE I. Barrier energies for selected PTCDA-on-inorganic semiconductor diodes using thermionic emission and diffusion models.

Inorganic substrate	Majority-carrier type	J/J_{TE} [a]	$q\phi_{Bp}$ (eV)		ΔE_v [b] (eV)
			TE	diffusion	
Si	n	2.0×10^{-4}	0.61 ± 0.01	0.39 ± 0.01	...
	p	1.4×10^{-4}	0.75 ± 0.02	0.56 ± 0.02	0.50 ± 0.02
Ge	p	6.6×10^{-5}	0.55 ± 0.03	0.30 ± 0.03	0.25 ± 0.04
GaSb	p	1.2×10^{-4}	0.60	0.37	0.29 ± 0.04
	n	3.9×10^{-5}	ohmic	ohmic	...
GaAs	n	5.2×10^{-5}	0.64	0.39	...
	p	1.4×10^{-4}	0.75	0.52	0.43 ± 0.05
InP	n	5.5×10^{-5}	0.55	0.30	...

[a] Values at $T = 300$ K, with $\langle v_c \rangle = 500$ cm/s.

[b] ΔE_v for p-type substrates only. For these calculations $m^* = m_0$ for PTCDA. The value for p-Si is measured; whereas for other materials, ΔE_v is calculated using ϕ_{Bp} obtained from Ref. 2 and reproduced here. Doping of p-Si and p-GaSb: 5×10^{15} cm^{-3}; p-Ge: 5×10^{14} cm^{-3}; and p-GaAs: 2×10^{16} cm^{-3}.

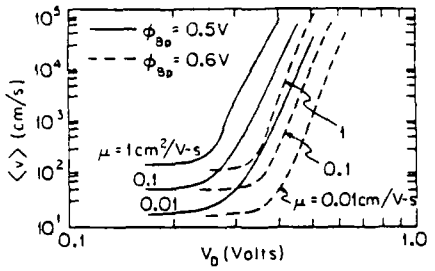

FIG. 9. Mean carrier velocity ($\langle v_c \rangle$) vs voltage across the substrate for OI-HJ diodes using organic thin films with different mobilities, and assuming barrier heights of 0.5 and 0.6 V. For these curves, a film thickness of 1000 Å and a hole lifetime of 1 μs are assumed.

swept across the organic film and collected at the metal contact, or else they recombine with injected holes arriving at the OI interface from the metal contact. In either case, this leakage current density is determined by the rate at which minority carriers are generated within the inorganic semiconductor.

Turning now to the carrier velocity in the inorganic substrate, Eq. (14) must be solved to obtain the diffusion velocity, v_d. Assuming that the doping density in the substrate (N_A) is uniform, the potential $\psi(x)$ (see Fig. 1) is parabolic. Thus:

$$\psi(x) = qN_A(W_D - x + t)^2/2\kappa_s + \Delta_s/q\,, \tag{21}$$

where κ_s is the semiconductor permittivity. Substituting this into Eq. (14) gives[11]

$$v_d \cong D_{ps}/2L_D = \mu_{ps}kT/2qL_D\,, \tag{22}$$

where $\mu_{ps} \cong 600$ cm^2/V s is the hole mobility in the (Si) inorganic material, and $L_D \sim 1000$ Å is the Debye screening length.[10] From this expression, we obtain $v_d \sim 10^6$ cm/s at room temperature.

One additional characteristic velocity of the OI diode is the hole drift velocity in inorganic semiconductor, which limits the rate at which holes can transit the depletion region under reverse bias. For most cases, this approaches the saturation velocity of holes in p-type semiconductors, which is typically between 5 and 10×10^6 cm/s.

Thus, we find that under nearly all bias regimes, the OI diode satisfies the condition that $\langle v_c \rangle / v_d \ll 1$. Furthermore, due to the large range over which $\langle v_c \rangle$ can vary for a small change in bias near $V_D = 0$, we have the circumstance that the OI diode changes its behavior from "Schottky-like" under large forward bias, to a "MIS-like" regime under small forward and reverse voltages. Under large reverse voltage, the device enters a "heterojunctionlike" regime whereby minority-carrier generation in the semiconductor substrate is balanced by recombination at the OI interface, thereby preventing charge inversion. The "heterojunction" regime also allows for Zener, or avalanche breakdown to occur at the largest applied reverse voltages.[7]

The characteristics of these various modes of OI-HJ operation are summarized in Table II. In the table, p_s refers to the density of holes at the OI interface, which is calculated in Sec. IV. The last column labeled "organic conductivity" gives a qualitative description of the current transporting nature of the thin film in each of the various bias regimes. More discussion of this unusual character of the OI-HJ is presented in Sec. V.

TABLE II. Operating regimes for organic-on-inorganic semiconductor heterojunctions.

Regime	Voltage range[a]	Current density	$\langle v_c \rangle$ (cm/s)	p_s	Organic conductivity
Schottky	$-V_a \gg \phi_B$	$J \gg J_s$	10^4–10^6	$\gg p_0$	SCL
MIS	$\lvert V_a \rvert \lesssim E_g/q$	$J \lesssim J_s$	~100–10^4	$\lesssim p_0$	leaky insulator
HJ	$V_B < V_a \ll \phi_B$	$J \sim J_s$	100–10^3	$\ll p_0$	ohmic

[a] Positive voltage refers to reverse bias for p-type substrates.

IV. QUASI-FERMI LEVELS

To calculate the position of the quasi-Fermi level (or imref) within the organic thin film, we employ:

$$E_{Fp}(x) - E_{v0} = kT\log[N_{v0}/p(x)]\,, \tag{23}$$

where N_{v0} is the valence-band effective density of states [cf., Eq. (16)], and E_{v0} is the energy of the valence-band maximum (or HOMO) in the organic film. In Fig. 10, $E_{Fp}(x) - E_{v0}$ is plotted as a function of x, where $p(x)$ is obtained with the aid of Eqs. (3)–(5). This function dips toward the valence-band maximum at the metal anode [i.e., $E_{Fp}(0) \to E_{v0}$], increasing to a nearly constant value as the OI interface is approached. By examining the position of the imref at $x = t$, we see that while V_0 increases from 5 mV in the ohmic regime to 100 mV in the SCL regime (Fig. 3), $E_{Fp}(t) - E_{v0}$ changes by only 30 meV. That is, the relationship between the imref position at the OI interface, and the voltage applied to the thin film (V_0), is sublinear. Furthermore, under reverse bias, the conduction mechanism within the thin film is nearly always ohmic in nature, suggesting that V_0 is generally less than 10 mV for all bias levels of interest. Therefore, it can be concluded that under reverse, or even moderately large ($\lesssim 0.7$ V) forward biases, the imref position at the organic side of the OI-HJ is only a weak function of voltage dropped across the layer. This is consistent with assertions[4] that the occupancy of traps in equilibrium with the thin film does not change significantly with bias, and hence their contribution to total diode admittance is generally small.

To calculate the imref in the inorganic substrate, we assume that the doping is uniform, in which case the potential distribution, $\psi(x)$, is given by Eq. (21). Substituting Eq. (21) into Eq. (11), and using Eq. (23) (with N_{vs} substituted for N_{v0}) one then obtains:

$$E_{Fp}(x) - qV_D = kT\ln\left(1 - \frac{\exp(-\beta)D(\theta/\beta)\exp(\theta^2\beta)[1 - \exp(qV_D/kT)]}{v_d/\langle v_c \rangle + D(\sqrt{\beta})}\right), \tag{24}$$

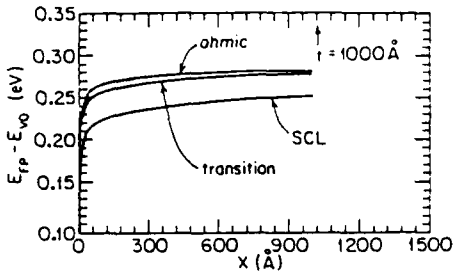

FIG. 10. Quasi-Fermi energy (E_{Fp}) vs position within the organic film for several different bias regimes. Parameters used in this calculation are the same as those in Fig. 3.

where the normalized position is $\theta = (W_D + t - x)/W_D$, and[20]

$$D(\sqrt{\beta}) = \exp(-\beta)\int_0^{\beta} \exp(t^2)dt$$

$$= \sqrt{\beta}\exp(-\beta)\sum_{n=0}^{\infty}\frac{\beta^n}{(2n+1)n!}. \quad (25)$$

Here β is the band bending parameter, given by

$$\beta = -q[\psi(W_D) - \psi(t)]/kT. \quad (26)$$

To determine E_{Fp} at the semiconductor surface, Eq. (24) is solved at $\theta = 1$, giving:

$$E_{Fp}(t) - qV_D = kT\ln\left(\frac{v_d/\langle v_c\rangle + D(\sqrt{\beta})\exp(qV_D/kT)}{v_d/\langle v_c\rangle + D(\sqrt{\beta})}\right). \quad (27)$$

This is similar to the result obtained for Schottky barrier diodes,[11] except that $\langle v_c\rangle$ is the mean carrier velocity in the organic layer rather than the collection velocity in the metal, and V_D is used in place of V_a.

It is apparent that the magnitude of $v_d/\langle v_c\rangle$ determines the functional dependence of E_{Fp} on voltage. For example, under forward bias where $V_D < 0$, and where $v_d/\langle v_c\rangle$ is large (as is the case for most OI diodes, see Sec. III), Eq. (27) reduces to $E_{Fp}(t) - qV_D = 0$. That is, the imref is flat throughout the substrate, independent of voltage, thereby allowing the majority-carrier imref in p-type diodes to sweep through the lower half of the band gap with V_a. Under reverse bias, $V_D > 0$, implying that $E_{Fp}(t) - qV_D = 0$ as long as the second term in the numerator of Eq. (27) is smaller than $v_d/\langle v_c\rangle$. For small reverse biases, this is indeed the case in OI diodes. On the other hand, for Schottky diodes where $v_d/\langle v_c\rangle \cong 1$, the second term dominates at almost all applied voltages. In this latter case,

$$E_{Fp}(t) - qV_D = -qV_D, \quad (28)$$

which results in the surface imref being "pinned" to its value at $V_D = 0$.

Returning to Eq. (27), we can calculate the potential at the inorganic side of the OI-HJ as a function of V_D using the values determined for $\langle v_c\rangle$ in Sec. III. The surface potential (Fig. 1) is just

$$q\psi(t) = q\psi_s = E_{Fp}(t) + q\phi_{Bp}. \quad (29)$$

In Fig. 11, ψ_s is plotted versus V_D for both forward ($V_D < 0$) and reverse ($V_D > 0$) bias. This function is determined for several barrier heights. For comparison, it is also plotted for a Schottky barrier device, where $v_c \sim 10^6$ cm/s. It can be seen that the surface potential for a Schottky barrier diode is essentially constant under reverse bias, as expected from diffusion and thermionic emission theory.[11] On the other hand, ψ_s decreases linearly with V_D under forward bias. For this reason, the Schottky diode is useful for exploring traps which are located between the equilibrium Fermi level and the majority-carrier band edge, as has been suggested by Barret and co-workers.[21,22] This is due to the ability to "scan" the imref through the trap energies by changing the applied voltage, and hence altering the net trap occupancy.

In the case of the OI diode, the carrier velocity, $\langle v_c\rangle$, is several orders of magnitude less than v_d. Thus, the surface potential varies linearly with V_D in both forward and reverse bias over nearly the entire band gap of the inorganic semiconductor, as shown in Fig. 11. This result is largely independent of hole mobility within the organic film, as long as the mobility is in the range typical of organic crystalline solids[23] (i.e., $\mu_p < 10$ cm^2/V s). However, if the barrier height is sufficiently small, the surface potential cannot be brought near to the minority-carrier band edge due to the increased leakage currents. Under forward bias, the behavior of the surface potential is identical to that of the Schottky barrier device, i.e., it decreases linearly with applied voltage.

Finally, Fig. 12 is a plot of the free-hole concentration in the inorganic material at the OI interface [see Eq. (12)]. The same parameters employed in Fig. 11 are also used in this figure. The surface charge concentration is seen to vary over fourteen decades as the potential changes from a forward bias of -0.5 V (where $p_s \cong 10^{15}$ cm^{-3}), to a reverse bias of 0.5 V (with $p_s = 1$ cm^{-3}). The surface charge density can be understood directly in terms of the carrier velocity. For example, under strong forward bias $\langle v_c\rangle$ is large, resulting in a hole transit time which is small compared with τ_{p0}. In this case, p_s must be very large. However, as $\langle v_c\rangle$ is reduced, τ_{p0} becomes small with resepect to the transit time, thereby depleting the thin film of injected charge near the OI interface.

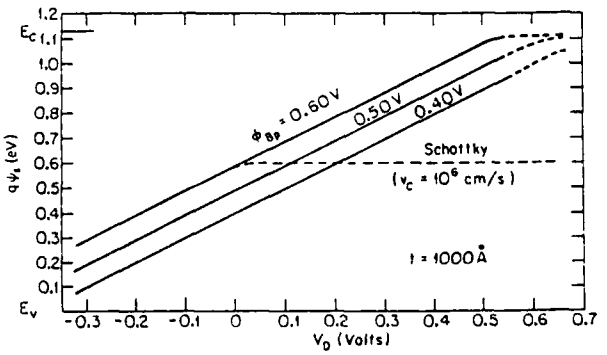

FIG. 11. Potential at the inorganic semiconductor surface as a function of voltage across the depletion region for OI-HJ diodes with several different values of barrier energy. The surface potential for a Schottky barrier diode (with barrier energy of 0.6 eV) is shown for comparison.

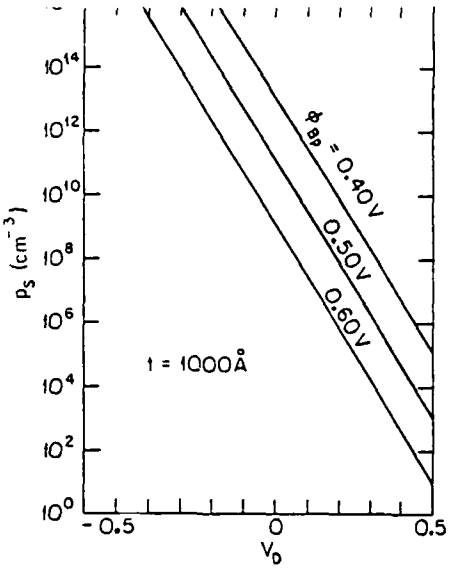

FIG. 12. Hole concentration (p_s) at the OI-HJ interface as a function of voltage for the same parameters used in Fig. 11.

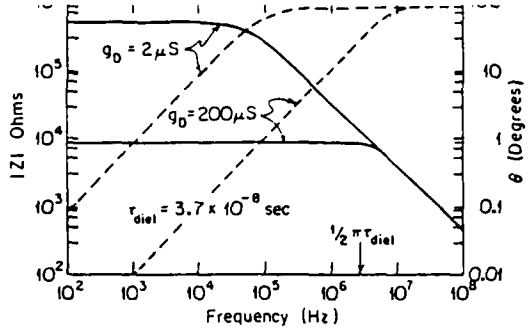

FIG. 13. OI-HJ impedance ($|Z|$, solid lines) and phase angle (θ, dashed lines) vs frequency. A dielectric relaxation time of 37 ns is assumed for the organic thin film. These functions are calculated for two values of barrier conductance: $g_D = 2$ and 200 μS, the latter value corresponding to a "leaky" diode. Also, a depletion region capacitance of $C_D = 5$ pF is assumed.

V. DISCUSSION AND CONCLUSIONS

A significant result of this work is that the transport theory presented in Sec. II results in an expression for diffusion-limited current in OI-HJ diodes from which an accurate barrier energy, and hence ΔE_v, for these novel heterojunctions can be determined. Several experimental results have also been presented which corroborate the theoretical treatment. In addition, we have shown that the majority-carrier quasi-Fermi level in OI-HJ diodes is flat throughout the bulk of the inorganic semiconductor substrate for small forward and reverse bias voltages. Thus, applying a bias to the OI-HJ causes the majority-carrier imref to sweep through nearly the entire semiconductor bandgap. Provided that the density of surface states at the OI-HJ is small ($\lesssim 10^{12}$ cm^{-2} eV^{-1}), these states will be thermalized as E_{Fp} is lowered below the trap energy, and thus will contribute to diode admittance.[4,5] A higher surface state density can result in Fermi level pinning at the OI-HJ, thereby leading to nonlinear, and hence difficult to determine relationships between the applied voltage V_a, the voltage dropped across the substrate V_D, and E_{Fp}.

The dependence of the quasi-Fermi level on voltage results from the relatively low carrier velocities and carrier concentrations in the organic thin film. By calculating both E_{Fp} and $\langle v_c \rangle$ as a function of V_D, we find that the OI-HJ has unique electrical properties as compared with conventional inorganic semiconductor devices. For example, near $V_D \cong 0$, there is only a small voltage drop across the organic film, and the film can be considered similar to a leaky insulator. Thus, the device at low voltages behaves like a MIS capacitor whose impulse response is limited by the thin-film dielectric relaxation time, $\tau_{diel} = \kappa_0/\sigma$. Here σ is the conductivity of the film, and is typically[7] $\sigma \sim 10^{-5}$ S/cm. Using[7] $\kappa_0 = 0.37 \times 10^{-12}$ F/cm, we obtain $\tau \cong 37$ ns. Hence, under reverse or low forward voltages, the OI-HJ diode varies from a resistive response at $f < 1/2\pi\tau_{diel} \cong 5$ MHz (depending on the inorganic semiconductor depletion capacitance C_D) to a reactive response at higher frequencies. The impedance and phase versus frequency characteristics of a typical OI diode operated in the MIS regime is illustrated in Fig. 13, assuming a conductance for the OI-HJ barrier (g_D) of 2 or 200 μS. The latter value corresponds to a "leaky" OI-HJ with a low barrier potential, ϕ_{Bp}. In this case the organic film can be approximated by a resistor-capacitor network in series with a resistor due to the HJ, whose characteristic time is τ_{diel}. As the network becomes reactive ($\theta > 45°$), then $|Z| \propto 2\pi fC$, which decreases inversely with frequency. For less leaky barriers (e.g., $g_D = 2\,\mu$S), the network is in series with capacitance C_D, and hence becomes reactive at frequencies lower than $2\pi\tau_{diel}$.

Under large forward bias, the diode performs analogous to a Schottky diode. In this case, a large charge density (p_{inj} or n_{inj}) is injected from the substrate and metal contacts into the thin film such that n_{inj} or $p_{inj} \gg p_0$. Here, conduction in the organic material becomes extrinsically space-charge limited. This effectively "pulls" the Fermi energy to the organic band edge, hence making the organic material degenerate. With the exception that the resistance of the thin film in this regime is a nonlinear function of voltage, in most other respects the film behaves as if it were an ohmic metal contact forming a Schottky barrier with the substrate. In the Schottky regime, the carrier velocity $\langle v_c \rangle$ can be as high as 10^4–10^5 cm/s. With a film thickness of 100 Å, a response time of between 10 and 100 ps would result.

Finally, a third "heterojunction" regime is obtained under moderate to large reverse bias voltages. The poor insulating properties of the organic material prevent the OI-HJ interface from being strongly inverted. Hence, under reverse bias this charge must either recombine at the interface within the bulk of the film, or diffuse to the ohmic metal contact made to the film surface. As the bias is further increased, large electric fields are developed in the semiconductor substrate, leading to eventual bulk breakdown in the inorganic

material.[8] Note that when large breakdown currents are developed, charge transport is once more limited by space-charge effects in the organic material, similar to conditions of large forward bias.

ACKNOWLEDGMENTS

The authors thank the Rome Air Development Center, the Joint Services Electronics Program, the Powell Foundation, and the Air Force Office of Scientific Research without whose support this work could not have been accomplished.

[1]F. Capasso and G. Margaritondo, Eds., *Heterojunction Band Discontinuities: Physics and Device Applications* (North-Holland, Amsterdam, 1987).
[2]P. H. Schmidt, S. R. Forrest, and M. L. Kaplan, J. Electrochem. Soc. **133**, 769 (1986).
[3]M. Ozaki, D. Peebles, B. R. Weinberger, A. J. Heeger, and A. G. MacDiarmid, J. Appl. Phys. **51**, 4252 (1980).
[4]S. R. Forrest and P. H. Schmidt, J. Appl. Phys. **59**, 513 (1986).
[5]S. R. Forrest, M. L. Kaplan, and P. H. Schmidt, J. Appl. Phys. **60**, 2406 (1986).
[6]F. F. So and S. R. Forrest, J. Appl. Phys. **63**, 442 (1988).
[7]S. R. Forrest, M. L. Kaplan, and P. H. Schmidt, J. Appl. Phys. **55**, 1492 (1984).
[8]M. Lampert and P. Mark, *Current Injection in Solids* (Academic, New York, 1970).
[9]F. F. So, S. R. Forrest, H. L. Garvin, and D. J. Jackson, Technical Digest of Integrated and Guided Wave Optics Conference, Santa Fe, March 28–30, 1988.
[10]S. M. Sze, *Physics of Semiconductor Devices*, 2nd ed. (Wiley, New York, 1981).
[11]C. R. Crowell and M. Beguwala, Solid-State Electron. **14**, 1149 (1971).
[12]S. R. Forrest, M. L. Kaplan, and P. H. Schmidt, J. Appl. Phys. **56**, 543 (1984).
[13]C. R. Crowell, W. G. Spitzer, L. E. Howarth, and E. E. LaBate, Phys. Rev. **127**, 2006 (1962).
[14]M. A. Haase, M. A. Emanuel, S. C. Smith, J. J. Coleman, and G. E. Stillman, Appl. Phys. Lett. **50**, 404 (1987).
[15]R. H. Fowler, Phys. Rev. **38**, 45 (1931).
[16]S. R. Forrest, M. L. Kaplan, and P. H. Schmidt, Annu. Rev. Mater. Sci. **17**, 189 (1987).
[17]A. G. Milnes, *Deep Impurities in Semiconductors* (Wiley, New York, 1973).
[18]W. Warta, R. Stehle, and N. Karl, Appl. Phys. A **36**, 163 (1985).
[19]W. Warta and N. Karl, Phys. Rev. B **32**, 1172 (1985).
[20]This is known as Dawson's integral; see M. Abramowitz and I. Stegun, *Handbook of Mathematical Functions* (Dover, New York, 1965), p. 298.
[21]C. Barret and A. Vapaille, J. Appl. Phys. **50**, 4217 (1979).
[22]C. Barret, F. Chekir, and A. Vapaille, J. Phys. C **16**, 2421 (1983).
[23]F. Gutman and L. E. Lyons, *Organic Semiconductors* (Wiley, New York, 1967).